LBL-29155
UC-210

Lawrence Berkeley Laboratory
UNIVERSITY OF CALIFORNIA

APPLIED SCIENCE DIVISION

Technology Base Research Project for Electrochemical Energy Storage: Annual Report for 1989

May 1990

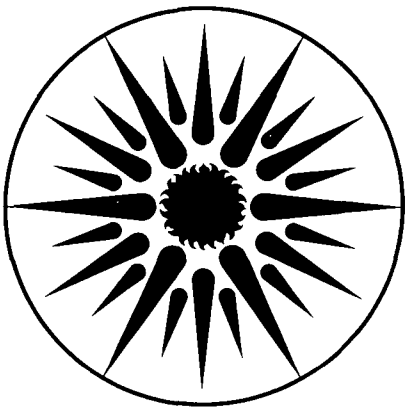

APPLIED SCIENCE DIVISION

Prepared for the U.S. Department of Energy under Contract Number DE-AC03-76SF00098.

DISCLAIMER

LBL-29155

TECHNOLOGY BASE RESEARCH PROJECT FOR ELECTROCHEMICAL ENERGY STORAGE

ANNUAL REPORT FOR 1989

Applied Science Division
Lawrence Berkeley Laboratory
1 Cyclotron Road
Berkeley, California 94720

Edited by Kim Kinoshita, Technical Manager

May 1990

This work was supported by the Assistant Secretary for Conservation and Renewable Energy, Office of Energy Storage and Distribution, Energy Storage Divison of the U.S. Department of Energy under Contract No. DE-AC03-76SF00098.

CONTENTS

EXECUTIVE SUMMARY

The U.S. Department of Energy's Office of Energy Storage and Distribution provides continuing support for an Energy Storage Program, which includes R&D on advanced electrochemical energy storage and conversion systems. A major goal of this program is to develop electrochemical power sources suitable for application in electric vehicles and/or electric load-leveling devices. The program centers on advanced secondary batteries and fuel cells that offer the potential for high performance and low life-cycle costs, both of which are necessary to permit significant penetration into commercial markets.

The DOE Electrochemical Energy Storage Program is divided into two projects: the Exploratory Technology Development and Testing (ETD) Project and the Technology Base Research (TBR) Project. The ETD Project management responsibility has been assigned to Sandia National Laboratory (SNL), and the Lawrence Berkeley Laboratory* (LBL) is responsible for management of the TBR Project. The ETD and TBR Projects include an integrated matrix of research and development efforts designed to advance progress on several candidate electrochemical systems. The role of the TBR Project is to perform supporting research for the advanced battery systems under development by the ETD Project, and to evaluate new systems with potentially superior performance, durability and/or cost characteristics. The specific goal of the TBR Project is to identify the most promising electrochemical technologies and transfer them to industry and/or the ETD Project for further development and scale-up. This report summarizes the research, financial and management activities relevant to the TBR Project in CY 1989. This is a continuing project, and reports for prior years have been published; they are listed at the end of the Executive Summary.

General problem areas addressed by the project include identification of new electrochemical couples for advanced batteries, determination of technical feasibility of the new couples, improvements in battery components and materials, establishment of engineering principles applicable to electrochemical energy storage and conversion, and the development of air-system (fuel cell, metal/air) technology for transportation applications. Major emphasis is given to applied research which will lead to superior performance and lower life-cycle costs.

---

* Participants in the TBR Project include the following LBL scientists: E. Cairns, K. Kinoshita and F. McLarnon of the Applied Science Division; and L. DeJonghe, J. Evans, R. Muller, J. Newman, P. Ross and C. Tobias of the Materials and Chemical Sciences Division.

The TBR Project is divided into three major project elements: Exploratory Research, Applied Science Research, and Air Systems Research. Highlights of each project element are summarized according to the appropriate battery system or electrochemical research area.

EXPLORATORY RESEARCH

The objectives of this project element are to identify, evaluate and initiate development of new electrochemical couples with the potential to meet or exceed advanced battery and electrochemical performance goals. Research was conducted on high-temperature molten-salt cells based on Li-alloy negative electrodes and metal disulfide positive electrodes. These cells exhibit very high performance, ease of manufacture, and freeze-thaw capability. Two key issues for this technology are to stabilize the performance of the FeS_2 electrode and to develop corrosion-resistant containment materials.

- Argonne National Laboratory (ANL) has achieved over 400 h (175 cycles) of stable operation with a bipolar Li alloy/FeS_2 cell. Post-test analysis of the cell confirmed the acceptable integrity of the hermetic seal.
- ANL observed that comparable performance can be obtained with an "electrolyte-starved" upper-plateau Li alloy/FeS_2 cell (compared to a flooded-electrolyte cell) by altering the electrolyte to a LiCl-rich composition (*i.e.*, in mol%, 34 LiCl-32.5 LiBr-33.5 KBr). The higher ionic conductivity of the LiCl-rich electrolyte compensates for the reduced electrolyte volume that is present in the electrolyte-starved cell.

APPLIED SCIENCE RESEARCH

The objectives of this project element are to provide and establish scientific and engineering principles applicable to batteries and electrochemical systems; and to identify, characterize and improve materials and components for use in batteries and electrochemical systems. Projects in this element provide research that supports a wide range of battery systems — alkaline, metal/air, flow, solid-electrolyte, and nonaqueous. Other cross-cutting research efforts are directed at improving the understanding of electrochemical engineering principles, minimizing corrosion of battery components, analyzing the surfaces of electrodes, and electrocatalysis.

Alkaline Cells often use Zn as the negative electrode, and it is this electrode that typically limits the lifetime of these cells. Efforts are underway to identify electrode and electrolyte compositions

that will improve the cycle-life performance of the Zn electrode, and to determine the operating conditions that lead to Zn dendrite formation.

- LBL has implemented a one-dimensional, time-dependent model of the Zn/NiOOH cell which elucidates the cause of active material redistribution in the Zn electrode during cycling. This model predicts a higher current density at the top of the electrode, compared to the central portion of the electrode, which produces steep concentration gradients that lead to non-uniform Zn distribution in Zn/NiOOH cells.
- LBL has observed that the use of carbonate and fluoride anions in the electrolyte triples the cycle life of Zn/NiOOH cells, compared to cells containing standard 6.8 M KOH-0.6 M LiOH electrolyte. Cells that contain K_2CO_3 or KF in the alkaline electrolyte have exceeded 300 cycles, with only modest Zn redistribution.
- LBL has concluded from an analysis of experimental data that the initiation of mossy Zn originates from: *i)* increased local surface overpotential (result of the current distribution which is perturbed by the growth of nodules), and *ii)* increased hydroxide-ion concentration around a protrusion (result of the local increase in current density).

Zinc/Halogen Cells use flowing electrolytes to promote the transport of Zn ions across the cell and to remove halogen as the cell is charged. The cell performance is limited by the tendency of the electrodeposited Zn to assume unwanted shapes, and efforts are aimed at understanding the complex phenomena that control the Zn electrode morphology.

- Brookhaven National Laboratory (BNL) has used EXAFS (extended X-ray absorption fine structure) to detect the waters of hydration and tetrahedral $Zn(OH)_4^=$ species, but no ion-pairing with alkali ions in saturated zincate solutions was observed. On the other hand, EXAFS revealed that considerable ion-pairing occurs in poly(ethylene oxide) (PEO) electrolytes (*e.g.*, $ZnBr_2(PEO)_8$, $RbBr(PEO)_8$).
- Lawrence Livermore National Laboratory (LLNL) has published the results of their earlier study on the diffusion coefficient of $ZnCl_2$ solutions: J.A. Rard and D.G. Miller, "Ternary Mutual Diffusion Coefficients of $ZnCl_2$-KCl-H_2O at 25°C by Rayleigh Interferometry," *J. Solution Chem.* **19**, 129 (1990).

Improved Components for Alkali/Sulfur and Alkali/Metal Chloride Cells, such as superior alternatives to the β"-Al_2O_3 ceramic electrolyte and the high-temperature sulfur-polysulfide electrode for Na/S cells, stable Li-ion conductors for Li/S cells, optimized $NiCl_2$ electrodes for Na/$NiCl_2$ cells, and a class of organosulfur electrodes for low-temperature alkali-metal cells, are under investigation.

- LBL has obtained 350 cycles in a Li/PEO/RSSR cell (RSSR, R = aliphatic, aromatic, ethereal or fluorinated organic moiety) at 50-90°C, which demonstrated up to 89% cathode utilization at 90% voltage efficiency. These results correspond to a specific energy of 260 Wh/kg and specific power of 150 W/kg. At 100°C, the corresponding values are 200 Wh/kg and over 2400 W/kg with up to 96% cathode utilization during a 5-min discharge.
- LBL has developed an advanced mathematical model of the sulfur electrode in high-temperature Na/S cells. The model, consisting of a set of non-linear partial differential equations, describes the diffusion, migration, and convection processes that take place during operation of such a cell.
- ANL has observed that the addition of sulfur increases the utilization of Ni in Na/$NiCl_2$ cells. The sulfur appears to improve the utilization by increasing the surface area and pore diameter of the Ni metal matrix. A composite of 35-wt% glass (Na_2O-Al_2O_3-B_2O_3-SiO_2) and β″-Al_2O_3 was identified by ANL which yielded acceptable resistivity ~25 ohm-cm) at 250°C for use as an alternative solid electrolyte in Na/metal chloride cells.
- Massachusetts Institute of Technology (MIT) has observed that the addition of CaO improves the stability of Li_2O-CaO-B_2O_3 glasses in high-activity Li environments but results in a lower ionic conductivity. However, relatively high conductivity is retained by the simultaneous addition of LiCl.
- Stanford University has observed that the positive electrode in Na/metal chloride cells limits the power output from cells of the present design. Evidence was found for time-dependent changes in the chloroaluminate molten salt.

Corrosion Processes in High-Specific-Energy Cells are under investigation, and the aim is to develop low-cost container and current-collector materials for use in nonaqueous, alkali/sulfur, and other molten-salt cells.

- Illinois Institute of Technology (IIT) has investigated the deposition mechanism of Mo in FLINAK (LIF-NaF-KF molten salt). Cyclic voltammetric studies indicate deposition occurs by a 3-electron quasi-reversible process. IIT has successfully electrodeposited Mo_2C coatings on the internal surface of container cans for Na/S cells.
- Johns Hopkins University has observed that the impurities (as high as 10,000 ppm and mostly water) in technical-grade PC cause breakdown of the passive films that are formed on Fe and Ni in 0.5 M $LiClO_4$/PC.

Components for Ambient-Temperature Nonaqueous Cells, particularly metal/electrolyte combinations that improve the rechargeability of these cells, are under investigation.

- Case Western Reserve University (CWRU) has used Fourier transform infrared spectroscopy to detect the presence of carbonate species which form when Li reacts with CO_2 at low partial pressure (2×10^{-7} torr). The increase in the intensity of the absorption band at 1450 cm^{-1} with exposure time to CO_2 indicates a gradual increase in the amount of carbonate that forms.
- Jackson State University has observed by *in situ* Raman spectroscopy that the passive film formed on Zn electrodes in alkaline solution consists of $Zn(OH)_2$. Some of the $Zn(OH)_2$ gradually transforms to ZnO when the potential is maintained in the passive region.
- The University of Minnesota has fabricated a Na/poly(pyrrole) cell with poly(ethylene oxide) (PEO) polymer electrolyte by thin-film technology which showed steady performance for five charge/discharge cycles at the C/3 rate.
- The University of Pennsylvania is collaborating with the Energy Research Laboratory (Svendborg, Denmark) to characterize the electrochemical behavior of a new conducting polymer for rechargeable Li batteries. This polymer has the highest Li-ion conductivity at room temperature of any observed to date. Thermal analysis studies (DSC, TGA) indicate that the polymer is completely amorphous between –90 and 200°C, and only loses weight slowly between 40 and 100°C.
- SRI has developed a Li-ion conducting polymer from a poly(ethyleneimine) derivative which has one of the highest ionic conductivities (4×10^{-5} ohm^{-1} cm^{-1}) at room temperature reported so far.

Cross-Cutting Research is carried out to develop mathematical models of electrochemical systems, and to address fundamental problems in electrocatalysis and current-density distribution; solutions will lead to improved electrode structures and performance in batteries and fuel cells.

- LBL has developed a mathematical model of the Na/$FeCl_2$ battery that predicts the effects of the state of discharge, cell temperature, precipitation and dissolution rates of NaCl, and current density on the current-potential relationship during charge/discharge.
- LBL employed light-scattering techniques to investigate anodic film formation. From these measurements, it was possible to extract the near-to-far-angle spectral power density ratio and to determine the particle size of Ag_2O obtained by anodic oxidation of Ag in KOH.

- LBL has developed mathematical models of the chemical and physical processes occurring at electrode surfaces which aid in the interpretation of data obtained by photothermal deflection spectroscopy (PDS). These models have led to a new cell design that permits the use of a thin layer of electrolyte, which is required for measurements of infrared absorption spectra of reaction intermediates on electrode surfaces.
- LBL has observed that a polycrystalline Pt surface which is modified by electrodeposited Sn is a good electrocatalyst for methanol electro-oxidation in sulfuric acid. This surface showed enhanced electrocatalysis compared to a low-index single-crystal Pt with electrodeposited Sn.
- A surface renewal model was developed by LBL to predict hydrogen supersaturation levels over horizontal electrodes, it showed excellent agreement with experimental data for platinized electrodes.

AIR SYSTEMS RESEARCH

The objectives of this project element are to identify, characterize and improve materials for air electrodes; and to identify, evaluate and initiate development of metal/air battery systems and fuel-cell technology for transportation applications.

Metal/Air Cell Research projects address bifunctional air electrodes, that are needed for electrically rechargeable metal/air (Zn/air, Fe/air) cells; and novel alkaline Zn electrode structures, that could be used in either electrically recharged or mechanically recharged cell configurations.

- LBL has developed a quantitative method for determining the number of oxygenated carbon atoms in carbon black samples. The corrosion rate of these carbon blacks in alkaline electrolytes could be correlated to the concentration of oxygenated species.
- CWRU has observed that the pyrochlore, $Pb_2Ru_2O_{6.5}$, exhibits high activity for the 4-electron reduction of O_2 in alkaline solution. Unfortunately, in the anodic mode, the pyrochlore dissolves in the electrolyte. In other studies, CWRU used *ex situ* FTIR reflectance studies to show that Co tetramethoxyphenylporphyrins (CoTMPP) adsorbs on HOPG in different orientations, depending on the preparative procedure.
- The LBL-developed Zn/air cell (80-cm^2 electrode area) that contains a particulate Zn electrode has operated at current densities up to 148 mA/cm^2, yielding a maximum power of 105 mW/cm^2 (at 20% depth of discharge). Projecting these results to a 32-kWh battery suggests a specific power of 238 W/kg and a specific energy of 177 Wh/kg.

- Metal Air Technology Systems International (MATSI) has demonstrated that over 500 charge/discharge cycles can be obtained for Zn deposition in a reticulated Cu-foam structure. Zinc loadings of 100 mAh/cm^2 can be routinely deposited without dendrite formation.

Fuel Cell Research, managed by Los Alamos National Laboratory (LANL), includes research in several areas of electrochemistry, theoretical studies, fuel-cell testing, fuel processing, and membrane characterization. Major achievements of the fuel-cell program during 1989 are listed below:

- LANL has demonstrated that the use of "planarization" (*i.e.*, filling the gaps in the carbon cloth with carbon powder) prior to applying the Pt/C electrocatalyst yielded performance with low Pt loading (0.22 mg/cm^2) that was comparable to that obtained at higher Pt loading (0.45 mg/cm^2).
- LANL achieved current densities of over 2 A/cm^2 in polymer-electrolyte membrane (PEM) fuel cells with 50-μm thick Nafion. Performance losses at higher current densities are attributed to an increase in cathode overpotential.
- LANL has obtained a new membrane ("Membrane C", Chlorine Engineers Corporation, Japan) which shows good, reproducible performance in PEM fuel cells.
- Measurements of water mass balance in PEM fuel cells by LANL suggest that single cells operate with a large excess of liquid water, usually carried into the cell as an aerosol.
- LANL has observed that the anode performance with fuels which contain CO is a strong function of the fuel utilization. At high fuel flow rates (*i.e.*, low utilization) the performance degradation caused by 100-ppm CO is severe, whereas at low flow rates (*i.e.*, high utilization) the performance degrades slowly. These results suggest that the improvement at low flow rates may be caused by the interaction of CO and O_2 which permeates through the membrane. This effect is similar to that observed when O_2 is injected directly into the anode feed stream.
- BNL has investigated underpotential deposited (UPD) Cu and Pb on Pt as an electrocatalyst for methanol oxidation. XANES (X-ray absorption near-edge spectroscopy) studies indicated that these UPD species were present in the non-metallic state. EXAFS studies of pyrolyzed Fe-TMPP (900°C) and Co-TMPP (800°C) showed no evidence of any nitrogen present. These findings contradict other hypotheses on the role of nitrogen in O_2 reduction on pyrolyzed macrocycle electrocatalysts.

MANAGEMENT ACTIVITIES

During 1989, LBL managed 20 subcontracts and conducted a vigorous research program in Electrochemical Energy Storage. LBL staff members attended project review meetings, made site visits to subcontractors, and participated in technical management of various TBR projects. LBL staff members also participated in the following reviews, meetings, and workshops:

- EPRI, Solid Oxide Electrochemistry Workshop, EPRI, Palo Alto, CA, January 13, 1989
- Gordon Conference in Electrochemistry, Ventura, CA, January 15-20, 1989
- TBR Project Review Meeting, Washington, D.C., March 8, 1989
- High Energy Density/Power Density Power Sources Workshop, SRI International, Menlo Park, CA, March 29-30, 1989
- 175th Meeting of the Electrochemical Society, Los Angeles, CA, May 7-12, 1989
- Review Meeting for Aluminum/Air Battery Development, Washington, D.C., May 24, 1989
- Lead Center Coordination Meeting, Washington, D.C., May 25, 1989
- Mini Symposium on Electrochemical Energy Storage, Paul Scherrer Institute, Wurenlingen, Switzerland, May 29, 1989
- 72nd Canadian Chemical Conference and Exhibition, University of Victoria, Victoria, B.C., Canada, June 4-8, 1989
- 24th IECEC Meeting, Crystal City, VA, August 8-10, 1989
- Symposium on *The Frontier of Electrochemistry*, Kyoto, Japan, September 15-16, 1989
- 40th ISE Meeting, Kyoto, Japan, September 17-22, 1989
- Conference on *Advanced In Situ Observation of Electrode Surfaces and Electrode Kinetics*, Sapporo, Japan, September 25-26, 1989
- Na/S Battery Review Meeting, Albuquerque, NM, October 11-12, 1989
- 176th Meeting of the Electrochemical Society, Hollywood, FL, October 15-20, 1989
- ERC Zn/Br_2 Battery Review Meeting, Washington, D.C., November 2, 1989
- National AIChE Meeting, San Francisco, CA, November 5-10, 1989
- 9th Battery and Electrochemical Contractors' Conference, Washington, D.C., November 12-16, 1989
- Al/Air Battery Review Meeting, Painesville, OH, December 4-5, 1989
- JCI Zn/Br_2 Battery Review Meeting, Milwaukee, WI, December 6, 1989

MILESTONES FOR THE TECHNOLOGY BASE RESEARCH PROJECT

Milestones accomplished in Fiscal Year 1989 by the TBR Project include:

- "Use *in situ* microelectrode potential measurements to determine multicomponent electrolyte species concentrations in operating porous Zn electrodes"

Measurements with microelectrodes detected the redistribution of material during electrode cycling, and indicated that convective flow may be influencing the electrolyte concentration near the edge of the electrode during discharge but has less of an influence during charge.

- "Go/no-go decision to initiate subcontract with an industrial partner to develop high-temperature Li/FeS_2 cells"

LBL encouraged industrial companies to pursue R&D on Li/FeS_2 cells, but was not successful in placing a subcontract. The available funds for research on Li/FeS_2 cells from LBL were combined with those available for development of Li/FeS battery technology from DOE/OTS (see below).

- "Go/no-go decision to continue support of battery technologies involving alkali metal electrodes in ambient-temperature non-aqueous electrolytes"

On the basis of the review committee's recommendations from the TBR Project Review Meeting of December 1988 and analysis of the technology by LBL, the TBR Project decided to continue support of research on ambient-temperature Li cells. The projects at Johns Hopkins University, CWRU and University of Pennsylvania were continued.

- "Employ *in situ* video microscopy with improved resolution to observe the morphology of Zn electrodeposited from flowing alkaline electrolyte"

A video microscope was employed to investigate the deposition of Zn in flowing electrolyte. The optics and electronics were improved to allow a maximum magnification of 375X, and an area of 300 μm x 200 μm can be observed with a diffraction-limited resolution of 0.5 μm.

- "Initiate joint R&D program with DOE/Office of Transportation Systems to develop Li/FeS and Li/FeS_2 molten-salt battery technology for electric vehicle applications"

Because of shrinking budgets and the weak interest by industrial organizations to pursue small R&D projects, the TBR project combined its resources with the DOE/OTS in a joint program to develop molten-salt battery technology. An RFP was issued in April 1989, and a decision was made in October 1989.

- "Complete testing of separate discharge and charge cells for Zn dissolution and deposition in alkaline electrolyte"

The experiments at Pinnacle Research Institute have successfully demonstrated that dendritic Zn produced in a charge cell can be discharged in a separate cell.

- "Demonstrate a life of 100 cycles for an improved electrolyte-starved upper-plateau Li/FeS_2 cell having overcharge tolerance"

A prismatic cell (20 Ah, 100-cm^2) with a powder separator (65% LiCl-LiBr-KBr/35% MgO) operated for over 135 cycles and 1200 h.

- "Go/no-go decision to initiate research on high-conductivity electrochemical cell components"

Five proposals were received in response to an RFP for research to improve the high-rate performance of secondary cells by developing components that have higher conductivity that the state-of-the-art components. A subcontract was awarded to SRI International to investigate high-conductivity polymer electrolytes for rechargeable Li cells.

- "Apply *in situ* Raman spectroscopy to identify adsorbed precursor layers in the formation of anodic films on metal surfaces"

Cyclic voltammetry of Cu in 1 M KOH showed the formation of adsorbed oxygen and subsequent oxide formation at about -350 mV (*vs* Hg/HgO). This electrochemical event was observed by *in situ* Raman spectroscopy, as noted by the emergence of a Raman peak at 633 cm^{-1}.

- "Complete development of an analysis program to evaluate *in situ* EXAFS data for electrode/electrolyte interfaces"

A program was developed to analyze EXAFS data obtained from electrocatalysts in fuel cell electrolytes. Particular care was required to subtract the background absorption by the electrolyte.

- "Initiate EXAFS study of carbon-supported pyrolyzed macrocycles for fuel-cell electrocatalysts"

The structure of pyrolyzed Fe and CoTMPP supported on carbon black was investigated by EXAFS. The results indicate that monodispersed, nitrogen coordinated, Fe and Co atoms are the sites for electrocatalysis.

- "Demonstrate the versatility of Photothermal Deflection Spectroscopy over an extended wavelength region of the infrared spectrum"

A specially designed cell was constructed which uses a thin electrolyte layer to minimize infrared absorption. The spectra of a thin film of acrylic cast on a Cu substrate was successfully obtained by *in situ* PDS.

- "Go/no-go decision to initiate a subcontract with an industrial organization to develop PEM fuel cells suitable for transportation applications"

LANL has decided to award a 600K$ contract to International Fuel Cells Corporation to investigate design and manufacturing methods for low-cost fabrication of PEM fuel cell power plants.

- "Go/no-go decision to initiate tests to determine the effects of inorganic and organic impurities on PEM fuel-cell performance"

LANL recommended that studies be initiated to investigate the effects of impurities, such as halide ions, heavy metal ions and those originating from recast polymer, because there are some indications that impurities may be partially responsible for the irreproducibility in the performance of single cells.

- "Develop a hermetic feedthrough seal for high-temperature Li/FeS_2 cells"

A ceramic seal consisting of mixed chalcogenides was successfully tested for over 1000 h and 100 cycles at 400°C in a sealed monopolar Li/FeS_2 cell.

- "Develop and characterize improved $NiCl_2$ electrodes for high-performance Na/$NiCl_2$ battery applications"

ANL demonstrated that the addition of NaF or S improved the performance of $NiCl_2$ electrodes. Addition of 2-wt% NaF or S to the 18-vol% Ni electrode improved the utilization of active material and the charge/discharge rates at 260°C.

- "Develop a composite glass-ceramic Na^+-ion conducting electrolyte with resistivity <75 ohm-cm at 250°C for use in high-power Na/MCl_2 batteries"

A composite glass-ceramic electrolyte (in mol%: 40.88 Na_2O, 1.42 Al_2O_3 and 57.70 SiO_2) was identified which showed encouraging results. However, it discolored during use, which indicated that the glass in the composite may not contain sufficient Na_2O to have acceptable stability in contact with Na.

- "Define CO levels that can be tolerated in PEM fuel cells with low Pt loadings and with various other anode electrocatalysts"

LANL has determined that CO concentrations of up to 200 ppm in the hydrogen feed stream can be tolerated without performance loss with low-Pt loaded anodes (0.35-0.45 mg Pt/cm^2) when up to 4% air is injected in the anode compartment. The tests were conducted with PEM cells operating at 80°C with gas pressures of 3 atm for H_2 and 5 atm for O_2.

- "Go/no-go decision on the use of metal bipolar plates in PEM fuel cells"

LANL has decided to proceed with tests of metal bipolar plates in PEM fuel cells. This decision is based on the better sealing and thinner cells that are obtained with metal rather than graphite in bipolar plates.

ACKNOWLEDGEMENT

This work was supported by the Assistant Secretary for Conservation and Renewable Energy, Office of Energy Storage and Distribution, Energy Storage Division of the U.S. Department of Energy under Contract No. DE-AC03-76SF00098. The support from DOE and the contributions to this project by the participants in the TBR Project are acknowledged. The assistance of Ms. Susan Lauer for coordinating the publication of this report and Mr. Garth Burns for providing the financial data are gratefully acknowledged.

ANNUAL REPORTS

1. Technology Base Research Project for Electrochemical Energy Storage - Annual Report for 1988, LBL-27037 (May 1989).
2. Technology Base Research Project for Electrochemical Energy Storage - Annual Report for 1987, LBL-25507 (July 1988).
3. Technology Base Research Project for Electrochemical Energy Storage - Annual Report for 1986, LBL-23495 (July 1987).
4. Technology Base Research Project for Electrochemical Energy Storage - Annual Report for 1985, LBL-21342 (July 1986).
5. Technology Base Research Project for Electrochemical Energy Storage - Annual Report for 1984, LBL-19545 (May 1985).
6. Annual Report for 1983 - Technology Base Research Project for Electrochemical Energy Storage, LBL-17742 (May 1984).
7. Technology Base Research Project for Electrochemical Energy Storage - Report for 1982, LBL-15992 (May 1983).
8. Technology Base Research Project for Electrochemical Energy Storage - Report for 1981, LBL-14305 (June 1982).
9. Applied Battery and Electrochemical Research Program Report for 1981, LBL-14304 (June 1982).
10. Applied Battery and Electrochemical Research Program Report for Fiscal Year 1980, LBL-12514 (April 1981).

SUBCONTRACTOR FINANCIAL DATA – CY 1989

Subcontractor	Principal Investigator	Project	Contract Value (K$)	Term (months)	Expiration Date	Status in CY 1989*
EXPLORATORY RESEARCH						
Molten-Salt Cells						
Argonne National Laboratory	C. Christianson	Molten-Salt Cells	380	12	9-89	C
APPLIED SCIENCE RESEARCH						
Lawrence Berkeley Laboratory	E. Cairns, L. DeJonghe, J. Evans, R. Muller, J. Newman, P. Ross, and C. Tobias	Electrochemical Energy Storage	1800	12	9-89	C
Zinc/Halogen Cells						
Brookhaven National Laboratory	J. McBreen	Zn Morphology	100	12	9-89	C
Components for Alkali/Sulfur Cells						
Argonne National Laboratory	C. Christianson	Solid Electrolytes	150	12	9-89	C
Stanford University	R. Huggins	New Battery Materials	195	12	11-89	C
Corrosion Processes in High-Specific Energy Cells						
Illinois Institute of Technology	R. Selman	Corrosion Resistant Coatings	129	12	12-89	C
Johns Hopkins University	J. Kruger	Corrosion/Passivity Studies	80	13	8-89	C

Subcontractor	Principal Investigator	Project	Contract Value (K$)	Term (months)	Expiration Date	Status in CY 1989*
Components for Ambient-Temperature Nonaqueous Cells						
Case Western Reserve University	D. Scherson	Spectroscopic Studies	36	9	4-89	C
Jackson State University	H. Tachikawa	Raman Spectroscopy	47	12	12-89	C
University of Minnesota	W. Smyrl	Solid State Cells	95	12	7-89	T
University of Pennsylvania	G. Farrington	Polymeric Electrolytes	46	12	5-90	C
SRI International	D. Macdonald	Polymeric Electrolytes	97	12	6-90	C
AIR SYSTEMS RESEARCH						
Metal/Air Cell Research						
Case Western Reserve University	E. Yeager	Air Electrodes	196	11	5-90	C
Metal Air Technology Systems	R. Putt	Zn/Air Battery	119	12	1-90	C
Fuel Cell R&D						
Los Alamos National Laboratory	S. Gottesfeld	Fuel Cell R&D	1350	12	9-89	C
Brookhaven National Laboratory	J. McBreen	Fuel Cell Research	150	12	9-89	C

* C = continuing, T = terminating

PEO	poly(ethylene oxide)
PPY	poly(pyrrole)
PtQRE	platinum quasi-reversible electrode
PVP	polyvinylpyridine
RDE	rotating disk electrode
RMS	root mean square
SCE	saturated calomel electrode
SEM	scanning electron microscopy
SEXAFS	subtractive extended X-ray absorption fine structure
SNIFTIRS	subtractively normalized interfacial Fourier transform infrared spectroscopy
SNL	Sandia National Laboratories
SPE	solid polymer electrolyte
TBR	Technology Base Research
TDS	thermal desorption spectroscopy
TGA	thermal gravimetric analysis
TMPP	tetramethoxyphenyl porphyrin
U.P.	upper plateau
UPD	underpotential deposition
VLSI	very large-scale integration
XANES	X-ray near edge absorption spectroscopy
XPS	X-ray photoelectron spectroscopy

LIST OF ACRONYMS

AES	Auger electron spectroscopy
AIChE	American Institute of Chemical Engineers
ASIt	area specific impedance
AN	acetonitrile
ANL	Argonne National Laboratory
BNL	Brookhaven National Laboratory
CSPL	Chloride Silent Power Limited
CTE	coefficient of thermal expansion
CV	cyclic voltammetry
CVD	chemical vapor deposition
CWRU	Case Western Reserve University
DME	dimethoxyethane
DOE	U.S. Department of Energy
DSC	differential scanning calorimetry
EPRI	Electric Power Research Institute
ETD	Exploratory Technology Development and Testing
EW	equivalent weight
EXAFS	extended X-ray absorption fine structure
FIC	fast ion conduction
FLINAK	LiF-NaF-KF molten salt
FTIRRAS	Fourier transform infrared reflectance absorption spectroscopy
HOPG	highly ordered pyrolytic graphite
IAD	implicit alternating direction
IECEC	Intersociety Energy Conversion Engineering Conference
IIT	Illinois Institute of Technology
ISE	International Society of Electrochemistry
ISS	ion scattering spectroscopy
LANL	Los Alamos National Laboratory
LEED	low energy electron diffraction
LBL	Lawrence Berkeley Laboratory
MATSI	Metal Air Technology Systems International
MIT	Massachusetts Institute of Technology
OESD	Office of Energy Storage and Distribution
OPG	ordinary pyrolytic graphite
OTS	Office of Transportation Systems
PC	propylene carbonate
PDE	partial differential equation
PDS	photothermal deflection spectroscopy
PEM	proton-exchange membrane

II. EXPLORATORY RESEARCH

The major thrust of this project element is to evaluate promising electrochemical couples for advanced batteries for electric vehicles. The only advanced large-size electrochemical system that was investigated is based on a high-temperature Li molten salt cell. Novel components for various versions of rechargeable Li, Na, and Zn cells were also investigated, as described in the Applied Science section of this report.

A. MOLTEN-SALT CELLS

Molten-Salt Cells based on Li-alloy negative electrodes and metal disulfide positive electrodes can exhibit very high performance, ease of manufacture, and freeze-thaw capability.

Molten-Salt Li-Alloy/FeS_2 Cell Research

D.R. Vissers (Argonne National Laboratory)

The objective of this project is to develop advanced Li-alloy/FeS_2 cells with high performance ~200 Wh/kg and 400 W/kg), excellent cycle life (>1000 cycles), and low-cost fabrication. This research effort is focused on the development of overcharge-tolerant monopolar and bipolar cells which normally operate at temperatures of 375-425°C. Research topics addressed in 1989 include: *i)* demonstration of high performance and long life in overcharge-tolerant monopolar FeS_2 cells with MgO powder separators, *ii)* development and demonstration of a ceramic sealant for peripheral seals in bipolar cells and in feedthroughs of monopolar cells, and *iii)* verification of the performance improvements due to the bipolar configuration, *i.e.*, 30% higher specific energy and 100% higher specific power.

As reported previously (1), an improved monopolar Li-alloy/FeS_2 cell with the BN-felt electrode separator has exhibited high performance and long cycle life. This cell has a low-melting electrolyte, 25 mol% LiCl-37 mol% LiBr-38 mol% KBr (mp, 310°C), and a densely loaded FeS_2-15 mol% CoS_2 electrode, which is operated only on the upper-voltage plateau (U.P.). In this report period, the BN-felt separator was replaced with an MgO powder separator, which has the potential for lower costs and greater thermodynamic stability in overcharge-tolerant U.P. FeS_2 cells. However, the MgO powder separator, since it is not physically stable under flooded electrolyte conditions, must be operated in an "electrolyte-starved" cell configuration. To develop an electrolyte-starved, overcharge-tolerant cell, cells with LiAl + 10 mol% $Li_5Al_5Fe_2$/LiCl-LiBr-KBr/U.P. FeS_2 (22.5-Ah capacity) with 100-cm^2 MgO powder separators were fabricated and tested. These cells demonstrated performance comparable to that of the flooded cell with BN-felt separator. To increase the ionic conductivity of the electrolyte-starved cell, which is normally about 30% lower than that of the flooded cell, the electrolyte composition was shifted off-eutectic to a LiCl-rich composition (in mol%, 34 LiCl-32.5 LiBr-33.5 KBr), which has a 25% higher ionic conductivity than that of the eutectic at 425°C. This higher ionic conductivity approximately compensates for the reduced electrolyte content of the electrolyte-starved cell. Therefore, the area specific impedance (ASI_t) of the electrolyte-starved cells (1.1 ohm-cm^2) is comparable to that of the flooded cell (1.0 ohm-cm^2). The capacity utilization of the electrolyte-starved cells after more than 50 cycles (>85% at a discharge current density of 50 mA/cm^2) is now slightly greater than that of the flooded cell.

The effect of conductive additives to the positive electrode (NiS_2, CoS_2) was studied to evaluate the improvement in electrode performance in the LiCl-rich electrolyte. In cells containing the new electrolyte and no electrode additive, about 85% utilization of theoretical FeS_2 capacity was seen at the 50 mA/cm^2 discharge rate, and in general, utilization was only 10% lower than that seen in similar cells containing an additive. The impedance of an U.P. FeS_2 electrode without additive (see Fig. 1) was about 10-15% higher

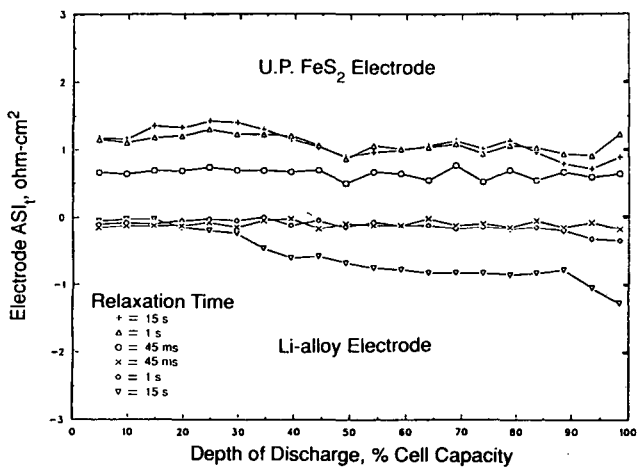

Fig. 1. Half-cell ASI_t measurements of electrolyte-starved U.P. FeS_2 cell (no additives) having LiCl-rich LiCl-LiBr KBr electrolyte at 425°C. (XBL 907-2323)

I. INTRODUCTION

This report summarizes the progress made by the Technology Base Research (TBR) Project for Electrochemical Energy Storage during calendar year 1989. The primary objective of the TBR Project, which is sponsored by the U.S. Department of Energy (DOE) and managed by Lawrence Berkeley Laboratory (LBL), is to identify electrochemical technologies that can satisfy stringent performance and economic requirements for electric vehicles and stationary energy storage applications. The ultimate goal is to transfer the most-promising electrochemical technologies to the private sector or to another DOE project (*e.g.*, SNL's ETD Project) for further development and scale-up.

Besides LBL, which has overall responsibility for the TBR Project, LANL, BNL and ANL participate in the TBR Project by providing key research support in several of the project elements.

- The TBR Project consists of three major elements:
- Exploratory Research
- Applied Science Research
- Air Systems Research

The objectives and the specific battery and electrochemical systems addressed by each project element are discussed in the following sections, which also include technical summaries that relate to the individual projects. Financial information that relates to the various projects and a description of the management activities for the TBR Project are described in the Executive Summary.

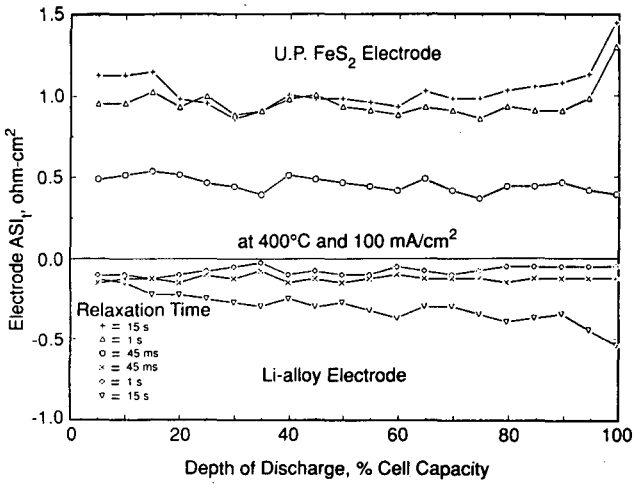

Fig. 3. Half-cell impedance measurements of electrolyte-starved U.P. FeS_2 cell operated at 400°C and 100 mA/cm². (XBL 907-2325)

high sulfur or Li activity. The mechanical strength of the sealant bond to various metals was evaluated metallographically to determine adhesion and wetting angles. Three substrate materials were examined: molybdenum, steel, and TiN-coated steel. In general, good-to-excellent wetting (*i.e.*, wetting angles from 25 to <10°) was observed. Sealant coverage was generally >95% of the available area. Metallographic examination of the sealant/substrate interface indicated excellent wetting on steel, with wetting angles approaching 0°. Efforts to improve sealing and bonding onto Mo have been quite successful. Initially, the sealant exhibited good wetting (25° wetting angle) on Mo, but the sealant tended to break away. However, a modified sealant was identified which displayed improved wetting and has a CTE of about 5.0×10^{-6}/°C, approximately that of Mo.

To verify the good performance of hermetic seals formed from the new materials, seals in both Li-alloy/U.P. FeS_2 monopolar and bipolar cell designs were tested. Chemical stability of the sealant materials was verified by post-test X-ray diffraction and differential thermal analysis. A feedthrough seal in a monopolar cell was successfully tested for over 1000 h and 100 cycles at 400°C. During this time, the seal maintained a resistance greater than 100 kohm, which is considered excellent for application in FeS_2 monopolar cells.

In the bipolar cell, the hermetic seal is formed at the periphery prior to cell assembly (Fig. 4). Here, a

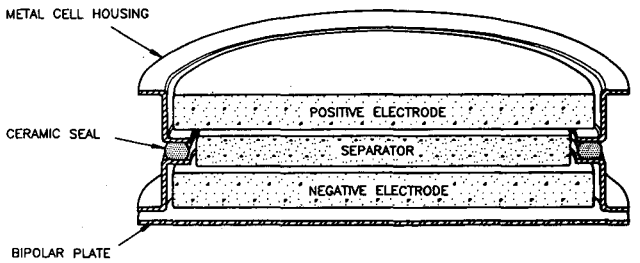

Fig. 4. Sealed bipolar cell design for Li-Alloy/FeS_x battery. Seal is formed prior to cell assembly. (XBL 907-2326)

ceramic ring is sealed to Mo on one side to form the FeS_2 electrode housing, and a steel assembly is sealed to the other side of the ring to form the Li-alloy electrode housing. In tests of the hermetic peripheral seal, a LiAl + 10 mol% $Li_5Al_5Fe_2$/U.P. FeS_2 bipolar cell (3-cm dia, 0.25-Ah capacity) was operated for over 175 cycles and 400 h, and exhibited high performance and >99% coulombic efficiency. Following 50 short discharge cycles, the U.P. FeS_2 electrode attained >80% utilization over the next 125 deep-discharge cycles. Cell capacity was limited by the negative electrode. Following voluntary termination, post-test analysis of the cell confirmed the stability of the metal-to-ceramic seals after 400 h of operation. The peripheral seal has been continually improved with over ten sealed bipolar FeS_2 cells tested thus far. A graded seal was developed with a CTE that approximately matched that of both the steel and Mo housings.

The performance of the bipolar FeS_2 cells is indicative of the benefits of the uniform current distribution across the surface of the electrode and the low internal impedance afforded by the bipolar cell configuration. The impedance of 0.65 to 0.75 ohm-cm² at 400°C which is obtained is about 1/3 less than that observed in monopolar prismatic cells. Further, the weight contribution of hardware to the cell is minimized by the bipolar design. The active material thus accounts for about 50% of cell weight for the bipolar cell, compared to about 30% for the monopolar prismatic FeS_2 cell. Calculations based on the electrode performance and component weight breakdown for a prototype cell (75-150 Ah capacity) indicate that the bipolar configuration should improve the specific energy by 30% and specific power by more than 100%. Additionally, the uniform current distribution in the bipolar battery configuration is expected to extend the cycle-life from 1000 to 2000 cycles.

(1.1 ohm-cm^2) than that of an electrode containing 10 mol% NiS_2 (0.9-1.0 ohm-cm^2). The increased impedance appears to be electronic in nature rather than ionic. That is, the ASI_t at 45 ms (electronic) is about 0.6 ohm-cm^2 for no additives, compared to 0.5 ohm-cm^2 with an additive of 10 mol% NiS_2. The ASI_t *vs* depth of discharge (DOD) curve for U.P. FeS_2 electrodes with and without additive remains flat during the bulk of the discharge, however. The electrolyte-starved U.P. FeS_2 electrode without conductive additives may have adequate performance for some applications, but noticeable improvement results from adding just 10 mol% NiS_2. Reducing the need for the CoS_2 additive is also being addressed in this research.

The recent development of overcharge-tolerant Li-alloy/FeS_2 cells was accomplished by application of a self-discharge mechanism, based on a "lithium-shuttle mechanism" (2,3). In general, the Li-shuttle mechanism involves diffusion of Li metal species across the separator to chemically discharge the positive electrode. The chief controlling element of the mechanism is the Li activity of the negative electrode, while the cell operating temperature and electrolyte composition are minor contributing factors. With this design, self-discharge rates of >2 mA/cm^2 develop at Li-alloy electrode potentials of –150 to –200 mV (*vs* alpha + beta Li-Al reference electrode). A Li Al_2Fe_2 alloy with a potential of –260 mV (*vs* alpha + beta Li-Al reference electrode) has been used in the engineering development of overcharge-tolerant cells.

Tests of overcharge-tolerant monopolar FeS_2 cells (25-Ah capacity) with reference electrodes (Ni/Ni_3S_2 have verified that the Li-shuttle mechanism provides sufficient levels of overcharge tolerance. Such cells have operated for more than 200 cycles with high performance and stable overcharge tolerance. In Fig. 2, the electrode potentials *vs* percent of capacity utilization for an U.P. FeS_2 cell [LiAl + 10 mol% $Li_5Al_5Fe_2$LiCl-LiBr-KBr (MgO)/FeS_2] are given for a single charge-discharge cycle. A bulk charge at 25 mA/cm^2 to 2.03 V was followed by a trickle charge of 3.0 mA/cm^2. As seen in Fig. 2, the Li-alloy electrode undergoes about a 200-mV transition near full-charge capacity. This is crucial to ensure cell longevity. The U.P. FeS_2 electrode shows a negligible change in potential during the overcharge period; that is, it is protected from the deleterious effects of overcharge polarization. The self-discharge rate undergoes a stepwise increase (a 20-fold increase by the Li-shuttle mechanism) to become equal and opposite in effect to the trickle-charge rate. In this test, the trickle-charge period (8 h) charged 15% more coulombs into the electrode than the rated capacity, and the extended trickle charge did not contribute to additional capacity in the subsequent discharge. A coulometric and galvanic analysis of the overcharge-tolerant cell design indicated ~0% charge acceptance for a trickle charge of 3.0 mA/cm^2 for the U.P. FeS_2 cell at 425°C.

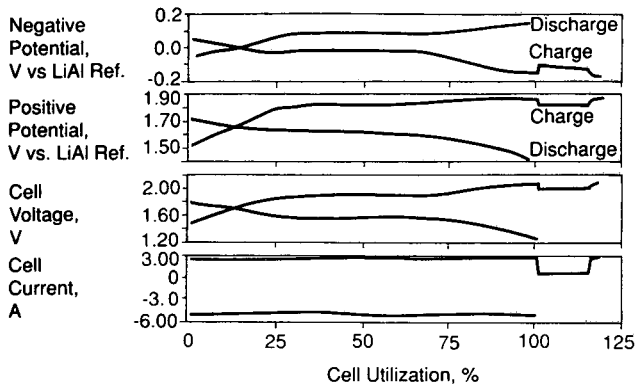

Fig. 2. Overcharge tolerance of U.P. FeS_2 cell operated at 425°C and overcharged by 15% at 3 mA/cm^2. No polarization of U.P. FeS_2 (positive) electrode indicates overcharge safeguard. (XBL 907-2324)

One electrolyte-starved, overcharge-tolerant LiAl + $Li_5Al_5Fe_2/FeS_2$ cell was fabricated with an electrode/MgO separator plaque that was pressed by Westinghouse Oceanic (Cleveland, OH). The performance of this cell at 425°C was outstanding: 92% utilization at a discharge current density of 50 mA/cm^2 and an ASI_{15s} of 1.2 ohm-cm^2. Concurrently, overcharge-tolerance tests indicated that 3-mA/cm^2 trickle charge rates were tolerated for over 10% additional charge capacity without positive electrode polarization. A near 100% coulombic efficiency was attained for normal charge-discharge cycles before and after the overcharge tolerance tests as seen in Fig. 3. The ASI_t curve for the positive electrode as a function of DOD was found again to be virtually flat out to 80% DOD. The impedance values observed at the different potential relaxation times (t = 45 ms to 15 s) indicate that ~50% of the electrode impedance is electronic rather than ionic. Such low cell impedance is highly desirable for power-demanding applications such as the electric vehicle. The demonstrated electrode performances support the projected specific energy of 175 Wh/kg and specific power of 200 W/kg for a 200-Ah prototype monopolar cell design.

Peripheral hermetic seals are required for the bipolar cell, while only a feedthrough seal is required for the monopolar cells. Hermetic seals for Li-alloy/FeS_2 cells were developed that were: *i)* electrically insulating, *ii)* gas tight, *iii)* compatible in coefficient of thermal expansion (CTE) with metal components, and *iv)* chemically stable in molten salts that have either

REFERENCES

1. T.D. Kaun (1985), *J. Electrochem. Soc.* **132**, 3063.
2. T.D. Kaun, T.F. Holifield, M. Nigohosian, and P.A. Nelson (1988), *174th Meeting of the Electrochemical Society*, Chicago, IL, Abstract No. 47.
3. L. Redey (1989), *J. Electrochem. Soc.* **136**, 1989.

PUBLICATIONS

1. L. Redey (1989), Chemical Overcharge and Overdischarge Protection for Li-Alloy/Transition-Metal Sulfide Cells, *J. Electrochem. Soc.* **136**, 1989.
2. D.R. Vissers, L. Redey, and T.D. Kaun (1989), Molten Salt Electrolytes for High Temperature Lithium Cells, *J. Power Sources* **26**, 37.
3. T.D. Kaun and P.A. Nelson, Molten-Salt Electrolyte Battery with Overcharge Tolerance, *U.S. Patent No. 4,851,306*, issued July 25, 1989.
4. L. Redey and P. A. Nelson, Overcharge Tolerant High-Temperature Cells and Batteries, *U.S. Patent No. 4,849,309*, issued July 18, 1989.
5. T.D. Kaun, T.F. Holifield, and W.H. DeLuca (1989), Lithium/Disulfide Cells Capable of Long Cycle Life, *Proc. of the Symp. on Materials and Processes for Lithium Batteries*, K.M. Abraham, ed., *176th Meeting of the Electrochemical Society*, Hollywood, FL, Vol. 89-4, p. 373.
6. T.D. Kaun, T.F. Holifield, M. Nigohosian, and P.A. Nelson (1989), Development of Overcharge Tolerance in Li/FeS and Li/FeS_2 Cells, *Proc. of the Symp. on Materials and Processes for Lithium Batteries*, K.M. Abraham, ed., *176th Meeting of the Electrochemical Society*, Hollywood, FL, Vol. 89-4, p. 383.
7. L. Redey (1989), Chemical Overcharge/Overdischarge Protection for Li-Alloy/Transition Metal Sulfide Cells, *Proc. of the Symp. on Materials and Processes for Lithium Batteries*, K.M. Abraham, ed., *176th Meeting of the Electrochemical Society, Hollywood*, FL, Vol. 89-4, p. 394.

III. APPLIED SCIENCE RESEARCH

The objectives of this project element are to provide and establish scientific and engineering principles applicable to batteries and electrochemical systems; and to identify, characterize and improve materials and components for use in batteries and electrochemical systems. Projects in this element provide research that supports a wide range of battery systems — alkaline, flow, molten salt, nonaqueous, and solid-electrolyte. Other projects are directed at research on improving the understanding of electrochemical engineering principles, corrosion of battery components, surface analysis of electrodes, and electrocatalysis.

A. ALKALINE CELLS

Zinc is often used as the negative electrode in alkaline cells, and it is this electrode that typically limits the lifetime of these cells. Efforts are underway to identify cell components that will improve the cycle-life performance of the Zn electrode.

Zinc Electrode Studies

E.J. Cairns and F.R. McLarnon (Lawrence Berkeley Laboratory)

The purpose of this research is to study the behavior of Zn electrodes used in secondary batteries, and to investigate practical means for improving their performance and lifetime. The approach used in this investigation is to study life- and performance-limiting phenomena under realistic cell operating conditions.

Mathematical Modeling. A one-dimensional, time-dependent model of the Zn/NiOOH cell has been fully implemented. This model is designed to elucidate the cause of active material redistribution in the Zn electrode, and it takes into account transport of electrolyte species, heterogeneous chemical reactions, kinetics, and local variations in current density. The model has simulated 20-50 deep-discharge cycles to study the effects of different processes on the rate and extent of Zn redistribution. These simulations have provided useful insight into the effects of non-uniform current distribution. With a current density at the top edge of the electrode about 10% greater than the average value, the rate of movement of Zn material at the top of the electrode is much greater and exhibits a stronger spatial variation, compared to the central region of the electrode. As the cell is cycled, the region of Zn material non-uniformity slowly extends to the lower portion of the electrode, although the rate of change is slower than that at the top of the electrode. Also, the non-uniform current density distribution results in steeper concentration gradients, so diffusion and migration processes become more important near the top edge of the electrode. Species movement through the separator tends to be significantly more rapid than transport in the direction parallel to the plane of the separator. However, in the areas of higher current density, the transport rate may not be high enough to replenish the reacting species, and concentration polarization can occur. The model results exhibit a strong dependence on the value of the rate constants used for the ZnO chemical dissolution/precipitation reactions

Optical Studies. Optical probe beam deflection is being used to measure electrolyte concentration gradients in a model Zn pore electrode. During 1989, the experimental apparatus was improved to permit a continuous range of cell dimensions to be studied. This was accomplished by employing a sub-micrometer-precision translation stage to control the height of the electrolyte compartment (which corresponds to the pore diameter). Also, the entire mounting and control system was rebuilt to closer tolerances. Several constant-current experiments were carried out with the new apparatus. The resulting probe beam deflection data were converted to refractive index gradients in two directions: parallel to and perpendicular to the plane of the electrode surface. As expected, the parallel gradients were strongest near the mouth of the pore electrode (the side nearest the counter electrode). The direction of these gradients as well as their relative magnitudes was successfully predicted by a one-dimensional numerical model of the transient diffusion processes in this system. This model is currently being refined to incorporate more-accurate values of the optical properties of the electrolyte, which were measured during 1989. The refractive index gradients normal to the electrode surface were also measured. The steady-state values of these gradients provide a measure of the current density profile along the electrode surface. This profile, when incorporated into the numerical model, provided good agreement between the experimental results and the model. Attempts to induce solid Zn species precipitation (known to occur in actual pores) in the electrolyte were successful only at current densities

much higher than those anticipated in a rechargeable Zn cell discharged at modest rates. Precipitation was monitored with optical microscopy, and studies of precipitation by scattering of the optical probe beam are now being conducted.

Cycling of Zn/KOH/NiOOH Cells. Cycle-life performance of the Zn/KOH/NiOOH cell is seriously degraded by Zn electrode active material redistribution (shape change) resulting from migration of Zn across the face of the negative electrode and to the positive electrode. This process can be retarded by two-fold reductions in electrolyte alkalinity, with a consequent four-fold reduction in zincate-ion solubility. Alternate anions can be substituted for hydroxyl ions in order to maintain adequate ionic conductivity in these modified electrolytes. Employing carbonate and fluoride anions triples cell cycle life, compared to standard 6.8 M KOH-0.6 M LiOH electrolyte. During 1989, several cells using reduced-alkalinity electrolytes approached or exceeded a goal of >300 cycles while maintaining >60% of initial capacity. A test cell containing 2.5 M KOH-2.5 M K_2CO_3-0.5 M LiOH electrolyte reached 334 cycles. *In situ* imaging x-rays showed that the Zn electrode was still quite uniform at the end of life. Dendritic shorting incidence was only about half that in standard cells. A wide range of alkaline-carbonate concentrations was evaluated. A cell containing 6.8 M KOH-1.75 M K_2CO_3-0.5 M LiOH electrolyte has reached 300 cycles at 63% capacity, indicating that even a low concentration of carbonate added to the standard electrolyte dramatically improves cell lifetime. An alkaline-fluoride cell (3.5 M KOH-3.3 M KF electrolyte) has achieved 400 cycles at >70% capacity with only modest Zn redistribution. Another approach to slowing Zn redistribution is to reduce zincate solubility by complexing it with $Ca(OH)_2$. Cells constructed with 25-mol% Ca electrodes do well in standard electrolyte, but attempts to cycle them in alkaline-carbonate or alkaline-fluoride electrolytes have been generally unsuccessful. The failure of Ca-containing electrodes to form efficiently in these electrolytes probably results from preferential formation of $CaCO_3$ or CaF_2 instead of $CaZn_2(OH)_6$. Work has begun on the development of sealed cells with the preparation of cell cases having pressure transducer attachments, and the computer-controlled cell cycling system has been adapted to monitor cell pressures. Early sealed-cell experiments show that the Zn electrode is producing small but significant amounts of H_2, and new electrode formulations are being investigated to suppress this unwanted phenomenon.

PUBLICATIONS

1. F.R. McLarnon and E.J. Cairns (1989), Energy Storage, *Annual Review of Energy*, **14**, Annual Reviews, Inc., Palo Alto, CA, pp. 241-71. LBL-26416.
2. E.J. Cairns and F.R. McLarnon (1989), Advanced Power Sources for Electric Vehicles and Stationary Energy Storage Systems, *175th Meeting of The Electrochemical Society*, Los Angeles, CA, Abstract No. 322.
3. J. Weaver, F.R. McLarnon, and E.J. Cairns (1989), Investigation of a Zinc Model Pore Electrode Using Photothermal Deflection Spectroscopy, presented at the *40th Meeting of the International Society of Electrochemistry*, Kyoto, Japan, Abstract No. 19-05-08-K.
4. T.C. Adler, F.R. McLarnon, and E.J. Cairns (1989), Improved Cycle-Life Performance with Alkaline-Carbonate Electrolytes in Zn/NiOOH Cells, presented at the *175th Meeting of The Electrochemical Society*, Hollywood, FL, Abstract No. 5.

Surface Morphology of Metals in Electrodeposition

C.W. Tobias (Lawrence Berkeley Laboratory)

The objective of this project is to develop a pragmatic understanding of the detail processes and their interactions in the macrocrystallization of metals necessary for the design and optimization of rechargeable galvanic cells. Studies related to the surface morphology of metals include observation of thick deposits for groove patterns in flow cells and at rotating disk electrodes (RDEs). Deposit topography is measured by a Taylor-Hobson profilometer, while more-detailed images of surface structure are obtained by scanning electron microscopy (SEM) and transmission electron microscopy (TEM). Electrolyte properties, including transport coefficients, are obtained by classical methods Observations on nucleation frequency as a function of electrode overpotential are performed on RDEs, using steady-state and transient techniques. A special flow cell, equipped with the capability to take time-lapse photographs and real-time video recordings, is used to observe and record macroscopic crystal growth and the development of characteristic patterns in the electrodeposition of Zn. Microprofiled Pt electrodes, on which predetermined surface roughness elements are grafted by very large-scale integration (VLSI) process technology, serve as reproducible substrates for the study of propagation of patterns in

macromorphology. Growth of surface profiles is modeled using finite difference-finite element or boundary element-techniques for solution of the Laplace equation.

A blocking mechanism for inhibitor action was demonstrated to be a reasonable alternative to the absorption mechanism of leveling. The main assumption underlying this mechanism is that the electrode area blocked by inhibitor is unavailable for electrocrystallization of metal ion. Thus the effective current density for metal electrodeposition is increased when compared to the apparent current density. Plots of the fraction of the surface blocked as a function of the flux ratio of inhibitor to metal ion reveal a line of positive slope through the origin; the slope is very close to the ratio of the electrode area blocked by a single inhibitor molecule to the size of the depositing metal ion. Using this mechanism for inhibitor action, a leveling simulation has been developed and used to investigate the effects of the shape of the mass transfer boundary layer on the transport of inhibitor to a microprofile. The shape of the boundary layer depends on the angle between the flow direction near the microprofile and the waviness of that profile. Two limiting angles were investigated: *a)* flow parallel to, and *b)* flow normal to the wave profile. Satisfactory qualitative agreement was found between the model and published experimental data. To provide more-reliable experimental observations, electrodes with precisely defined microprofiles were manufactured. Silicon was found to be the most suitable material available that was both optically flat and easy to pattern. Using silicon processing techniques developed for the manufacture of micromechanical devices, precise (70°) angular notches with depths from 30 to 70 μm have been prepared at the UCB Microlaboratory. For electrodeposition studies, a thin Au or Cu layer is first vapor-deposited on the microprofiled Si surface.

To understand how random protrusions grow into striations, micropatterned electrodes were designed to study the role of enhanced mass transfer on the microscopic scale. The experiments conducted show that the morphology of the resulting electrodeposit at long times is strongly dependent on the condition of the initial surface. Both nodules and ridges were investigated, leading to thin striae in the first instance, and much thicker striae under conditions identical to the second, respectively. Using a digital profilometer designed to measure a wide range of deposit thicknesses (1-250 μm) with minimal distortion, the development of striae with increasing charge passed was tracked. The analysis of the data used Fourier analysis and correlation techniques to find preferred striation frequencies. At short times, a Gaussian distribution of wavelengths is observed. When a critical amount of charge is passed, certain wavelengths become more pronounced close to the electrode leading edge. These wavelengths are equal to (or are multiples of) the visually observed striation wavelength. The striae propagate downstream rather quickly and cover the electrode. Under some conditions, striae also emerge close to the trailing edge, and the two meet with interesting and unexpected results. Flow channeling leads to converging streamlines, and the Fourier spectrum reflects this by increased power shifted to slightly higher frequencies.

The development of non-adherent, mossy Zn deposits adversely affects the cycle life of Zn secondary batteries. Based on fragmentary evidence obtained in this laboratory and elsewhere, the reasons for moss initiation are as follows: *i)* the current distribution is perturbed by the growth of nodules, leading to an increase in the local surface overpotential, and *ii)* the local increase in current density causes increased hydroxide-ion concentration near a protrusion, which, in turn, shifts the Zn deposition potential resulting in the nucleation of crystals with a different crystalline habit. Zinc deposits were characterized using TEM and energy dispersive x-ray spectroscopy. The selected area electron diffraction patterns show that mossy Zn is a crystalline phase without oxide inclusions. This result was confirmed using energy dispersive x-ray spectroscopy, which indicated that there was no difference in oxide concentration between the mossy and the compact parts of the electrodeposit. The magnitude of the oxide concentration corresponded to an approximately 0.5-nm thick surface layer, which can easily be attributed to exposure to air. Mossy Zn forms in both saturated and unsaturated flowing zincate electrolytes. Composition of the supporting electrolyte may be an important factor in determining the thickness of the compact layer before moss formation is initiated. When the KOH concentration is raised from 3 to 12 M, the compact layer thickness drops from 10 to 2 μm, indicating that hydroxide-ion buildup may contribute to the formation of moss. At a constant current density, raising the fraction of the limiting current causes the compact layer to become thicker. Likewise, when a constant flow rate is used, raising the fraction of the limiting current delays the onset of moss formation, a result that can be explained in the same manner. Using profilometry and roughness analysis, it has been found that both the average and root-mean surface roughness increase drastically just before mossy Zn is formed. There appears to be a critical value of the roughness parameter, 0.10 μm, that must be attained

before moss formation is initiated. The SEM shows that moss is initiated around large protrusions on the compact layer.

PUBLICATIONS

1. L. McVay, R.H. Muller, and C.W. Tobias (1989), Application of Videomicroscopy to *In Situ* Studies of Electrodeposition, *J. Electrochem. Soc.* **136**, 3384.
2. K.S. Jordan and C.W. Tobias (1989), The Role of Convection in Electrodeposition into Microscopic Trenches, LBL-20342.
3. K.S. Jordan and C.W. Tobias (1989), Leveling Caused by Inhibitors; A Theoretical Study, LBL-28343.

B. ZINC/HALOGEN CELLS

Flowing electrolytes are used in Zn/halogen cells to promote the transport of Zn^{++} across the cell and to remove halogen as the cell is charged. The cell performance is limited by the tendency of the electrodeposited Zn to assume unwanted shapes, and efforts are aimed at understanding the complex phenomenon that control the Zn electrode morphology.

Zinc Electrode Morphology

J. McBreen (Brookhaven National Laboratory)

The objectives of this research are to: *i)* increase the capacity density of zinc/bromine batteries, *ii)* develop stable Zn electrodes, *iii)* improve the efficiency of zinc/bromine batteries, and *iv)* develop *in situ* spectroscopic techniques for the study of battery materials. In 1989, research was conducted on *in situ* EXAFS (extended X-ray absorption fine structure) studies of zincate-ion complexes, ionically conducting polymers, and nickel oxide electrodes.

EXAFS Studies of Zincate-Ion Formation. Earlier investigations showed that identical EXAFS spectra were obtained for supersaturated zincate solutions and solutions with equilibrium solubility of zincate ions. The Fourier transform of the EXAFS had a large peak below 0.2 nm which corresponded to that expected for a tetrahedral $Zn(OH)_4^=$ species. However there was another peak at about 0.3 nm. This could be due to formation of zincate polymers, ion-pairing with the alkali ion or waters of hydration around the zincate species. A series of critical experiments were done to distinguish between these possibilities. This included EXAFS studies of $Zn(OH)_2$ and zincate in 12 M solutions of NaOH, KOH, RbOH and CsOH. Analysis of these results eliminated the possibility of either polymer formation or ion-pairing with the alkali ion. The second peak is due to waters of hydration around the zincate species. Additives such as silicate do not stabilize the zincate species but rather stabilize the supersaturated solutions by inhibiting precipitation.

EXAFS Studies of Polymer Electrolytes. EXAFS studies were done on $RbBr(PEO)_8$ and $ZnBr_2(PEO)_8$ in the temperature range from 25 to 120°C. Electrolytes were made from dry components and moisture was excluded during preparation, storage, and during the EXAFS measurements. The results indicate that there is considerable ion-pairing in the electrolyte even at 120°C. Data analysis of the results for $ZnBr_2(PEO)_8$ indicate that at 120°C the Zn-O coordination number is 5.63 and the coordination distance is 0.217 nm. The Zn-Br coordination number was 1.64 and the coordination distance was 0.233 nm. Reduction in ion-pairing would require modification of the dielectric properties of the electrolyte.

EXAFS Studies of the Nickel Oxide Electrode. During the year an extensive EXAFS study of the nickel oxide electrode was completed. This included *in situ* studies at steady state and time-resolved measurements coupled with cyclic voltammetry. The structure of the charged material (NiOOH) was elucidated for the first time. One surprising result of the time-resolved measurements was that on the anodic sweep considerable charge was passed before structural changes were observed in the EXAFS measurements. Sudden structural changes occurred at the anodic peak of the cyclic voltammogram. This is consistent with mechanisms that have been proposed in the past that involve the incorporation of OH- into the lattice. The reactions are

$$Ni(II) \rightarrow Ni(III) + e^-$$

$$Ni(III) + OH^- \rightarrow Ni(II) + [OH]$$

This could explain the excess charge that is often seen in these electrodes.

PUBLICATIONS

1. J. McBreen, W.E. O'Grady, G. Tourillon, E. Dartyge, A. Fontaine and K.I. Pandya (1989), *In Situ* Time Resolved XANES Studies of Nickel Oxide Electrodes, *J. Phys. Chem.* **93**, 6308.
2. J. McBreen (1989), The Nickel Oxide Electrode: Structure and Performance, *176th Meeting of the Electrochemical Society*, Hollywood, FL, Abstract No. 17.

3. J. McBreen, W.E. O'Grady, G. Tourillon, E. Dartyge and A. Fontaine, K.I. Pandya (1989), EXAFS Studies of Zincate Complexes in Alkaline Electrolyte, *176th Meeting of the Electrochemical Society*, Hollywood, FL, Abstract No. 8.

C. COMPONENTS FOR ALKALI/SULFUR CELLS

Superior alternatives to the β"-Al_2O_3 ceramic electrolyte and high-temperature sulfur-polysulfide electrode for Na/S cells, and stable components for Li/S cells are under investigation.

Electrochemical Properties of Solid Electrolytes

L.C. DeJonghe (Lawrence Berkeley Laboratory)

The objective of the current research program is to develop high-performance secondary batteries through advances in both solid electrolyte and novel electrode research. Earlier studies focused on the characterization of polycrystalline electrolytes such as β"-Al_2O_3. More recently the emphasis of the research has shifted to the evaluation of the electrical, physical, and chemical properties of a novel class of solid redox polymerization electrodes (SRPEs). These materials show extremely encouraging results as potential candidates for high-specific-energy, high-specific-power batteries.

A large number of organodisulfide polymers, $-(SRS)_n-$ were prepared and characterized. These polymers are generally synthesized by oxidation of dithio and/or polythio acids by suitable oxidants, *e.g.*,

$$n\ HS\text{–}R\text{–}SH + n\ I_2 \rightarrow -(SRS)_n- + 2n\ HI$$

The oxido-polymerization reactions are carried out in aqueous solution and are often quite rapid, going to completion in a few minutes to a few hours. The polymers are vacuum dried for several weeks prior to testing in solid-state cells.

Thin-film electrolytes and composite electrodes are cast from solution. Anhydrous acetonitrile, chloroform, tetrahydrofuran, and crystalline polyethylene oxide (PEO) of various molecular weights (3×10^5 to 5×10^6) are used for film casting. PEO-based electrolytes (10-100 μm) are cast from mixtures of a solution of PEO in acetonitrile (or other suitable solvent) and solutions of appropriate Li or Na salts, depending on the alkali metal anode to be used in the battery. Thin films of the organic cathodes (6-15 mg/cm^2) with surface capacities of 1 to 6 C/cm^2 are cast from solutions of PEO and redox polymers (with or without electrolyte salts) in an appropriate solvent or mixed solvents with dispersed carbon black. The thin films are dried under vacuum at 50°C for two days and subsequently kept under vacuum for a few weeks prior to testing.

Battery-grade Li foil (thickness = 25 to 100 μm) is obtained from Lithco Co. and stored in an argon-atmosphere dry box. Reagent-grade Na is highly purified by a previously published method prior to use. All-solid-state, thin-film, alkali metal/SRPE cells are constructed by sandwiching a polymeric electrolyte between the thin-film composite SRPE cathode and a thin foil of alkali metal; the cell is positioned between current collectors of matching stainless-steel plates.

The cell reaction for SRPE-based cells can be described for a simple case as

$$2n\ M + -(SRS)_n- = n\ M_2\ SRS$$

where M is an alkali metal (Li, Na, K) and R is an organic group. In the broader sense SRPEs can have more than two S groups per monomer R unit, and are reversible to other monovalent and divalent metals. In the fully charged state the SRPE electrode consists of a polydisulfide polymer that is depolymerized on discharge by scission of S-S bonds, leading to the formation of dithiolate salts in the fully discharged cell. The cells tested to date include both solid-state Li and Na cells, with theoretical specific energies in the range of 900 to 1500 Wh/kg.

Composite SRPEs consisting of polydisulfide polymers, polyethylene oxide (electrolyte), and dispersed carbon black were cycled in various cells including Na(liq)/β"-Al_2O_3/SRPE, Na(s)/PEO/SRPE, and Li(s)/PEO/SRPE. The Na(liq)/β"-Al_2O_3/SRPE cells clearly demonstrated the reversibility of solid-state polydisulfide electrodes to Na. The Na cells were cycled at 130 to 140°C at the 1.2C rate (2.0 mA/cm^2) for 40 to 50 cycles (80% of capacity) with no discernible deterioration with cycling. These cells also demonstrated rate capabilities of up to 6C rate (10 mA/cm^2) with close to 100% utilization of capacity and no evidence of adverse effects on electrode integrity, even under situations of abusive polarization on discharge or charge. Solid-state Na/PEO/SRPE and $Na_{3.75}Pb$/PEO/SRPE cells were also successfully cycled, attaining the highest current densities yet reported for solid-state Na cells. However, computer-driven four-probe DC techniques developed in this laboratory for isolating the various contributions to cell polarization show evidence for reaction of the Na electrode with the PEO solid electrolyte. This is not

observed with Li electrodes and may be due to the higher sensitivity of Na metal to impurities in the electrolyte such as water, solvent, etc.

All-solid-state batteries having Li anodes and SRPE cathodes have demonstrated the highest levels of performance to date for this system. One of the Li/PEO/SRPE cells has achieved 350 cycles in the temperature range of 50 to 90°C with a sustained specific energy of 260 Wh/kg (240 Wh/l), specific power of 160 W/kg (140 W/l), and up to 80% of cathode utilization at 90% voltage efficiency. At 100°C, specific powers of over 2400 W/kg at a specific energy of 200 Wh/kg have been achieved with up to 96% utilization of cathode capacity during a 5-min discharge. Furthermore, four-probe DC techniques show the Li/PEO and PEO/SRPE interfaces to be stable and essentially invariant with cycling.

PUBLICATIONS

1. S.J. Visco, C.C. Mailhe, L.C. DeJonghe, and M.B. Armand (1989), "A Novel Class of Organosulfur Electrodes for Energy Storage," *J. Electrochem. Soc.* **136**, 661.
2. M. Liu, S.J. Visco, and L.C. DeJonghe (1989), "Electrochemical Properties of Organic Disulfide/Thiolate Redox Couples," *J. Electrochem. Soc.* **136**, 2571.
3 S.J. Visco and L.C. DeJonghe (1989), "Sodium/Beta"-Alumina Batteries Operating at Intermediate Temperatures," *Mat. Res. Soc. Symp. Proc.* **135**, 553.
4. S.J. Visco, M. Liu, and L.C. DeJonghe (1989), "Ambient-Temperature High-Rate Lithium/Organosulfur Batteries," *176th Meeting of the Electrochemical Society*, Hollywood, FL, Abstract No. 60.
5. M. Liu, S.J. Visco, and L.C. DeJonghe (1989), "All-Solid-State, Thin-Film, Rechargeable Lithium Batteries with Novel Solid Redox Cathodes," *176th Meeting of the Electrochemical Society*, Hollywood, FL, Abstract No. 65; LBL-27964.
6. M. Liu, S.J. Visco, and L.C. DeJonghe (1989), "Electrochemical Investigations of a Class of Novel Redox Cathodes," *176th Meeting of the Electrochemical Society*, Hollywood, FL, Abstract No. 66; LBL-27963.
7. S.J. Visco, M. Liu, M.B. Armand, and L.C. DeJonghe (1989), "Novel High-Rate, Solid-State Lithium Batteries and Their Relationship to Protein Folding," *176th Meeting of the Electrochemical Society*, Hollywood, FL, Abstract No. 70.
8. M. Liu, S.J. Visco, and L.C. DeJonghe (1989), "Electrode Kinetics of Organodisulfide Cathodes for Storage Batteries," LBL-24906.

High-Temperature Cell Research

E.J. Cairns and F.R. McLarnon (Lawrence Berkeley Laboratory)

The objectives of this research are to investigate new electrodes, electrolytes, and other cell components, and to determine the fundamental mechanisms of capacity loss of the electrodes as well as means for eliminating the losses. Experimental studies of candidate materials for high-temperature cells are augmented by mathematical modeling of electrode behavior during cycling.

Mathematical Modeling. A comprehensive model of the sulfur electrode in Na/S cells has been developed. The cell being modeled is of the tubular central-Na type, and includes a thin layer of α-Al_2O_3 felt around the β''-Al_2O_3 solid electrolyte in order to prevent deposition of sulfur on the solid electrolyte during cell charge. The model consists of a set of nonlinear partial differential equations (PDEs) that describe the processes of diffusion, migration, and convection that take place during the operation of such a cell. Linearization of these highly nonlinear equations and their boundary conditions has been accomplished by implementation of a symbolic equations manipulator, written in "Mathematica." The Mathematica program automatically generates the corresponding banded matrices used in the Newman-IAD technique for solving time-dependent PDEs. This work results in a tremendous reduction of the tedious effort necessary to linearize the PDEs, and to generate the corresponding matrices necessary for numerical solution. Solution of the linearized equations is effected on a digital computer via implementation of the Newman-IAD method, which is a finite-difference technique for the solution of second order linear PDEs. Due to the mathematical complexity of the system, which involves the simultaneous solution of both elliptic and parabolic equations, with the character (elliptic or parabolic) at each point dependent upon the phases present, the numerical solution has been split into two stages: *a)* solution of the system in the one-phase region, and *b)* solution of the system in the two-phase region. Presently, the effort is directed towards *(a)* above, with work on *(b)* left for the future. An attempt will be made to predict the effect of various charge-discharge regimens upon cell operation.

Phosphorus/Sulfur Electrode Studies. The addition of phosphorus to the sulfur cathode in the Na/S cell may improve power output by reducing Na^+-ion transport resistance. We anticipate that the long-chain Na polysulfides that form in standard sulfur electrodes during discharge will be modified to

lower-molecular-weight species by phosphorus, which may act as a molecular chain terminator in this system. This would decrease the viscosity in the cathode melt, allowing faster transport of Na^+ ions in the melt, thereby decreasing cell overpotential and increasing its power output. An initial melting-point study has indicated that, in general, the Na-P-S system has a higher melting point than expected. Thus, an experimental cell that will permit the evaluation of optimal P/S ratios *via* equilibrium electromotive force (EMF) measurements at temperatures up to 500°C is being developed. The cell uses β''-Al_2O_3 electrolyte and is constructed much like standard Na/S cells. Phosphorus/sulfur ratios found to be promising in the EMF studies will be tested in a practical Na/S cell configuration, and performance will be compared with that of standard Na/S cells.

Sodium/Metal Chloride Cell Research

D.R. Vissers (Argonne National Laboratory)

The objective of this research is to generate the scientific and technical information needed to develop advanced Na/metal chloride (Na/MCl_2) cells with high specific energy (200 Wh/kg) and power (>200 W/kg). Despite the high theoretical specific energy (790 Wh/kg) of the $Na/NiCl_2$ cell, the performance of single β''-Al_2O_3 tube cells is limited to 125 Wh/kg and ~100 W/kg (1-11). The major research areas addressed in 1989 include: *i)* determining how temperature, sulfur additive, and porosity affect the performance of the $NiCl_2$ electrode, *ii)* developing thin $NiCl_2$ electrodes with very low resistance (0.5 ohm-cm^2) at 300°C, and *iii)* developing a glass/ceramic composite electrolyte with a resistivity of ~25 ohm-cm at 250°C. In addition, modeling design studies have indicated that high-performance $Na/NiCl_2$ cells (200 Wh/kg and 300-500 W/kg) can be developed by increasing the solid-electrolyte area of the cell.

The electrode studies have focused on increasing the performance of the $NiCl_2$ electrode because the electrochemistry of this electrode is simpler than that of $FeCl_2$ and its performance is superior as well. In these cell tests, the $NiCl_2$ electrode (30-40 mAh capacity) is located on the inside of the β''-Al_2O_3-tube electrolyte in an annular configuration. During the tests, the effects on performance of *i)* electrode porosity in annular electrodes (16, 18, and 20 vol% Ni), *ii)* sulfur additives (2 wt%), as used in the current technology, *iii)* cycling rates (charge and discharge rates of 2, 4, and 8 h), and *iv)* temperature (220, 260, and 300°C) were investigated. To improve the performance of this electrode, which represents about 50% of the cell weight, we are developing high-capacity-density electrodes, 0.50-0.55 Ah/cm^3, made from a sintered mixture of Ni and NaCl (3:1 capacity ratio). This capacity loading is almost 50% higher than that used in the current technology.

The results of these studies clearly indicated that charge rate, sulfur addition, electrode porosity, and temperature have a marked effect on electrode utilization. Those cells that were charged quickly tended to have lower utilizations than those charged more slowly. In some cases, the effect of charge rate was more pronounced than the effect of temperature on the electrode utilization. Sulfur seemed to increase the electrode utilization at all discharge rates. In cell studies conducted at 260°C and the 8-h charge rate, marked effects of the sulfur additive and the volume percent Ni used in the electrode were observed. For example, in the 18 vol% Ni electrode containing sulfur, there was a 95% utilization at the 2-h discharge rate, as compared to only 50% in the electrode without sulfur. Sulfur appears to improve the charge acceptance of the Ni electrode by increasing the surface area and pore diameter of the Ni metal matrix. The 16 and 20 vol% Ni electrodes did not perform as well as the 18 vol% Ni electrode, suggesting that electrode porosity is an important factor in electrode performance.

The area specific impedance of the 18 vol% Ni electrode with sulfur, which was the best-performing electrode in this study, was 1.2 ohm-cm^2 at 300°C. This value is nearly comparable to state-of-the-art cells, which have values of about 1.0-1.05 ohm-cm^2. In an effort to reduce their impedance, the electrodes were fabricated with larger mean pore diameters, which were obtained by altering the present fabrication procedure. Electrodes fabricated by this procedure tended to have significantly lower impedance, <0.50 ohm-cm^2 at 300°C.

Investigations were carried out on a nonporous Ni wire electrode to better understand the reaction mechanisms of the $NiCl_2$ electrode. This study showed that a $NiCl_2$ surface layer forms on the Ni during charge which limits the area capacity (C/cm^2) of the electrode. The area-capacity limit is in the range of 0.1-0.7 C/cm^2, depending on the conditions. A temperature increase from 205 to 386°C improves the area-capacity limit from 0.1 to 0.6 C/cm^2 (at 1 mA/cm^2). Based on these results, a model of the electrode which predicts the capacity density characteristics of the porous electrode and the effect of temperature has been developed and shown to agree very well with the porous electrode studies discussed above.

Research on composite electrolytes has focused on the development of a glass-β''-Al_2O_3 ceramic composite. The rationale behind this development is that advanced cell designs require high-surface-area multi-tube or prismatic electrolytes to reduce the voltage losses. The current material, β''-Al_2O_3, is difficult to fabricate into the prismatic configurations. Glasses, on the other hand, are easier to fabricate but do not have as high a conductivity. A composite of the two materials could possess the desired properties of both materials. On the basis of ionic conductivity and chemical stability, glasses in the Na_2O-Al_2O_3-B_2O_3-SiO_2 system were selected for testing in this work, and a resistivity value of 75 ohm-cm at 250°C was set as a target for the composite.

All Na_2O-Al_2O_3-B_2O_3-SiO_2/β''-Al_2O_3 composites contained about 35 vol% glass (50 wt%). The addition of more glass was found to increase the resistivity of the composite; while less glass produced a composite with very little strength. The composites were sintered at 1000°C to lessen soda loss (which occurs at the temperature needed to sinter β''-Al_2O_3, 1400°C). Glasses with no borate and small amounts of Al_2O_3 were found to produce better composites than glasses containing larger amounts of B_2O_3 and Al_2O_3.

Using the above results and the proper precursor preparation, composites with excellent resistivity values, ~25 ohm-cm at 250°C, were produced. Preliminary experimental results suggest that these materials may have acceptable chemical stability against Na. Future work in this area will be directed toward further optimizing the fabrication method and determining the performance of the composite in small cell tests.

In the cell modeling studies of the Na/MCl_2 system, three different cell design configurations were modeled to estimate the voltage-loss characteristics (IR drop) of these designs, and thus, their potential for high performance. The designs considered were the 100-Ah single tube design now being used in state-of-the-art cells, a multi-tube cell design, and a cell design using an array of flat-plate electrolyte structures that contain a number of individual square pocket electrode compartments, each of which is operated in parallel. To determine the voltage-loss characteristics of the three cell designs, literature values were used for the resistivity of β''-Al_2O_3 and area specific impedance values estimated from the published cell data for $NiCl_2$ electrodes with 0.25-0.35 Ah/cm^3 loading densities (3,4).

The results of this analysis indicated that the voltage losses can be decreased by more than an order of magnitude by shifting from a low-surface-area single tube to a high-surface-area multi-tube or flat-plate compartmented design. The projected specific energy and power for such high-surface-area cells is ~200 Wh/kg and 300-500 W/kg. While this initial design analysis clearly demonstrates the potential of the system, further work needs to be carried out to refine the calculations.

REFERENCES

1. J. Molyneux, C. Sands, S. Jackson, and I. Witherspoon (1987), *Proc. of the 22nd Intersociety Energy Conversion Engineering Conference*, Philadelphia, PA, p. 975.
2. R.J. Bones, J. Coetzer, R.C. Galloway, and D.A. Teagle (1987), *J. Electrochem. Soc.* **134**, 2379.
3. R.M. Dell and R.J. Bones (1987), *Proc. of the 22nd Intersociety Energy Conversion Engineering Conference*, Philadelphia, PA, p. 1072.
4. A.R. Tilley and R.M. Bull (1987), *ibid.*, p. 1078.
5 J.L. Sudworth, R.C. Galloway, and D.S. Dermott (1987), *Electric Vehicles* **73**, 14.
6. M.L. Wright and J.L. Sudworth (1987), *172nd Meeting of the Electrochemical Society*, Honolulu, HI, Abstract No. 103.
7 J. Coetzer (1986), *J. Power Sources* **18**, 377.
8. J. Coetzer and M.J. Nolte (1986), *U.S. Patent No. 4,592,969.*
9. R.J. Bones, J. Coetzer, R.C. Galloway, and D.A. Teagle (1986), *170th Meeting of the Electrochemical Society*, San Diego, CA, Abstract No. 763.
10 J. Coetzer and M.M. Thackeroy (1986), *U.S. Patent No. 4,288,506.*
11. J. Coetzer, R.C. Galloway, R.J. Bones, D.A. Teagle, and P. Mosely (1985), *U.S. Patent No. 4,546,005.*

PUBLICATIONS

1. I. Bloom and M.C. Hash (1989), "High-Conductivity Composite Electrolytes," *176th Meeting of the Electrochemical Society*, Hollywood, FL, Abstract No. 529.
2. I. Bloom, S.K. Orth, and D.R. Vissers (1989), "Effect of Some Design Parameters on the Performance of $NiCl_2$ Electrodes," *176th Meeting of the Electrochemical Society*, Hollywood, FL, Abstract No. 96.
3. L. Redey and I.D. Bloom, "Membrane Reference Electrode," *U.S. Patent No. 4,814,062*, March 21, 1989.
4. L. Redey and D. R. Vissers (1989), "Investigation of Ni/$NiCl_2$ Electrodes in Basic Chloroaluminate Melt," *176th Meeting of the Electrochemical Society*, Hollywood, FL, Abstract No. 95.

Electrical Conduction and Corrosion Processes in Fast Ion Conducting Glasses

H.L. Tuller (Massachusetts Institute of Technology)

The objective of this project is to develop highly conductive glasses with improved stability in high-Li-activity environments. The studies have focused on: *i)* the addition of stabilizing ions to bulk glasses, *ii)* the formation of chemically passive layers on highly conductive glass substrates, and *iii)* the transport properties of fast-ion-conducting (FIC) glasses. This project was completed in 1989.

The properties of two glass systems were investigated:

i) Boracites:

$$0.378[(1\text{-}x\text{-}y)Li_2O + x(LiCl)_2 + y\ CaO] \cdot 0.622B_2O_3$$

with x = 0.25 and 0.415.

ii) Metaborates:

$$0.49[(1\text{-}x\text{-}y)Li_2O + x(LiCl)_2 + y\ CaO] \cdot 0.49\ B_2O_3 \cdot 0.02\ Al_2O_3$$

with x = 0.15 and 0.4. The CaO content in these glasses varied between the limits y = 0-0.3, while the O/B ratio was maintained constant.

The conclusions of this study are as follows. The addition of CaO to Li_2O-LiCl-B_2O_3 FIC glasses leads to enhanced stability in Li environments. At least for the boracites, the effect is primarily kinetic. The addition of Ca apparently depresses the minority hole concentration in the ionic reaction layer leading to a decreased chemical diffusivity. Although Ca additions do tend to depress the Li^+ ion conductivity, relatively high values of conductivity can be retained in such systems by simultaneous additions of LiCl.

PUBLICATIONS

1. F.A. Fusco, M. Massot, M. Oueslati, E. Haro and H.L. Tuller (1989), "Structural Changes in Fast Ion Conducting Chloride Doped Potassium Borate Glasses," *Solid State Ionics* **135**, 189.
2. F.A. Fusco and H.L. Tuller (1989), "Fast Ion Transport in Glasses," in *Superionic Solids and Solid Electrolytes-Recent Trends*, A.L. Laskar and S. Chandra, eds., Academic Press, San Diego, CA, p. 43.
3. S.L. Fusco and H.L. Tuller (1989), "Lithium Ion Transport in Li_2O-LiCl-CaO-B_2O_3 Glasses," in *Proc. of the International Conference on Solid State Ionics*, Hakone, Japan.

New Battery Materials

R.A. Huggins (Stanford University)

The objective of this program is to develop materials for high-performance secondary batteries. The emphasis of the research is to understand the important structural, thermodynamic and kinetic properties of these materials which influence their behavior as cell components. An important aspect of this program is to understand the relationship between fundamental thermodynamic and kinetic parameters (*e.g.*, phase equilibria, Gibbs' free energy and chemical diffusion within solid phases, and the microscopic and macroscopic electrochemical phenomena) which influence the behavior of battery materials.

The effort in this project has focused on different aspects of alkali metal/metal chloride cells: *i)* characterization of electrode materials at elevated temperature, and *ii)* investigation of alternative intermediate-temperature electrolytes.

The studies of high-Na-activity alloys suggested that the number of alloys with desirable properties for use as negative electrode materials is somewhat limited compared with the analogous Li-based materials. Furthermore, the most useful materials appeared to be those that were alloyed with relatively heavy, non-transition metals (*e.g.*, Pb).

Some attention was given to obtaining a better understanding of the mechanistic aspects of the kinetic behavior of the positive electrode, which was observed to limit the power output of the cells of the current design. Evidence was found for time-dependent changes in the chloroaluminate molten salt.

PUBLICATIONS

1. R.A. Huggins (1989), "Materials Science Principles Related to Alloys of Potential Use in Rechargeable Lithium Cells," *J. Power Sources* **26**, 109.
2. A. Petric, S. Crouch-Baker, R.M. Emerson, T.M. Gur and R.A. Huggins (1989), "Thin Film Positive Electrodes for Lithium-Iron Sulfide Batteries Produced by Atmospheric Pressure Chemical Vapor Deposition," in *Proc. of the Symposium on Materials and Processes for Lithium Batteries*, K.M. Abraham and B.B. Owens, eds., The Electrochemical Society, Pennington, NJ, p. 101.

3. S. Crouch-Baker and R.A. Huggins (1989), "Composite Polyphase Electrochemical Cell Components," in *Proc. of the Symposium on Solid State Ionics*, G. Nazri, R.A. Huggins and D.F. Shriver, eds., Materials Research Society, Boston, MA, p. 177.
4. B.T. Ahn and R.A. Huggins (1989), "Synthesis and Lithium Conductivities of Li_2SiS_3 and Li_4SiS_4," *Mat. Res. Bull.* **24**, 889.

D. CORROSION PROCESSES IN HIGH-SPECIFIC-ENERGY CELLS

The aim of these projects is to develop low-cost containers and current-collector materials for use in nonaqueous, alkali-sulfur, and other molten-salt cells.

Corrosion-Resistant Coatings for High-Temperature High-Sulfur-Activity Applications

J.R. Selman (Illinois Institute of Technology)

The objective of this research is to develop corrosion-resistant coatings for cell components that are exposed to high-sulfur-activity environments in Li/FeS_2 and Na/S batteries. This research is directed at developing technology for the production of molybdenum, molybdenum carbide and titanium nitride coatings. Such coatings, which are obtained by electrochemical or chemical vapor deposition, are potential alternatives to present methods (*e.g.*, chromizing) of protecting the metal parts in high-temperature batteries.

Optimized Deposition of Mo and Mo_2. The main objective of this task during 1989 was to elucidate the mechanism leading to the nucleation and growth of dense layers of Mo and Mo_2C. Cyclic voltammetric (CV) studies indicated that Mo is deposited in a 3-electron quasi-reversible process with a subsequent chemical reaction that is specific to molten FLINAK, which partially redissolves Mo metal. In the highly alkaline zone close to the electrode surface such a reaction can produce oxyfluorides; this may explain why layers thicker than 5-7 μm, although still completely dense, are difficult to plate with high current efficiency. Chronopotentiometry indicates a quasi-reversible diffusion controlled process with the Mo product slightly soluble. The diffusion coefficient of Mo(III) at 600°C is estimated to be 7.3×10^{-5} cm^2/s.

Solutions of molybdate and carbonate in FLINAK produce reducible carbon as well as Mo, both of which are reduced in the same potential range, *i.e.*, between –1.6 and –1.8 V *vs* PtQRE. At 600°C these elements apparently do not react to form carbide. However, at 800°C and higher, electrodeposition is followed by chemical reaction to Mo_2C. In a subsequent anodic sweep, a single carbide decomposition peak is observed. Preliminary analysis of potential-step transients in a FLINAK-molybdate melt at 600°C indicates the growth of randomly nucleated two-dimensional centers. Addition of carbonate to this melt causes a second surface process, which appears to be the co-reduction of carbonate observed in CV experiments. At 750°C and higher, the instrument response time is inadequate to resolve the nucleation rate.

Preparation of Mo and TiN by PE-CVD. The apparatus assembled during the previous reporting period had to be remodeled to satisfy the safety requirements and to accommodate various types of reactive gases. Initial experiments are scheduled to start in 1990.

Corrosion Testing of Mo, Mo_2C and TiN Coatings. The stability of refractory coatings is currently determined in polysulfide melt at 330°C by cyclic voltammetry during a 100-h test. The main feature of this test is the dynamic polarization which simulates charge/discharge cycling in an actual Na/S cell. Thus far, tests have been carried out on small coupons coated with Mo, Mo_2C and TiN. Preparations have been made to test full-scale cans and current collectors with these coatings. Cell containers of 65-cm^3 volume for Na/S batteries have been internally coated with Mo_2C and supplied to CSPL (Runcorn, U.K.). Significant modifications were required to adapt the plating procedure to such large internal areas. Deposition of Mo_2C on 0.25-in diameter stainless steel rods for current collection in Li-alloy/FeS_2 batteries is in progress. These samples will be delivered and tested at ANL.

Corrosion, Passivity, and Breakdown of Allows Used in High-Energy Batteries

J. Kruger and P. Moran (The Johns Hopkins University)

The overall objective of this project is to investigate the phenomenon of passivation and its breakdown on metals and alloys in nonaqueous solvents for rechargeable Li batteries. The long-term integrity of the cell container and structural components is a critical issue that influences the lifetime of these batteries. In 1989, the work has focused on examining the corrosion behavior of 99.9985% Fe and 1018 carbon steel in anhydrous propylene carbonate (PC) solutions with 0.5 M $LiAsF_6$ and in PC with 0.5 M $LiClO_4$. The behavior of Fe and 1018 carbon steel was also examined in technical-grade PC to determine the influence of impurities in PC on the corrosion proc-

esses. Finally, the behavior of nickel (Ni 200) and 304 stainless steel in both anhydrous and technical-grade PC with $LiAsF_6$ was determined.

The oxidation of PC and the electrolytes are important factors in the passivation and corrosion behavior of alloys in these systems. The approximate oxidation potentials relative to the Li potential for these chemicals are: oxidation potential for PC (PC_{ox}) = 3.6 V (*vs* Li), oxidation potential for AsF_6^- = 5.1 V, oxidation potential for ClO_4^- = 4.5 V.

For Fe and 1018 carbon steel in PC with either electrolyte, the air-formed film is stable at potentials below PC_{ox}. If the air-formed film is removed mechanically, repassivation occurs quickly by adsorption of PC molecules. Above PC_{ox}, adsorption of PC can no longer provide protection as it is oxidized on contact with the electrode surface. Iron remains passive above PC_{ox} in $LiClO_4$ due to the formation of a protective salt film of $Fe(ClO_4)_2$, and it is passive all the way up to the oxidation potential of the perchlorate ions. In $PC/LiAsF_6$, however, Fe is not passive above PC_{ox} as the $Fe(AsF_6)_2$ salt film is more soluble. The 1018 carbon steel is not stable above PC_{ox} in either electrolyte. The higher solubility of $Fe(AsF_6)_2$ explains the behavior in $PC/LiAsF_6$, and sulfide inclusions in the 1018 carbon steel are responsible for its behavior in $PC/LiClO_4$. Pitting occurs predominantly at the inclusions indicating that they somehow interfere with the formation of the protective salt film. Approximately 500 ppm water or greater is sufficient to interfere with passivity, where it exists, in these systems. Also, passivity in these systems, where it exists, is lost in technical-grade PC which has impurities as high as 10,000 ppm (mostly water).

Nickel 200 has been examined in anhydrous and technical-grade PC containing 0.5 M $LiAsF_6$. With its air-formed film intact, Ni 200 is passive in both systems up to ~700 mV positive to the PC_{ox} potential. Pitting is observed in both solutions above this potential. The impurities in technical-grade PC cause an activation of the surface, as evidenced by an increase in the passive current density, but they do not cause premature breakdown of the passive film. It was also found that Ni 200 in technical-grade PC with $LiClO_4$ was stable up to 500 mV positive to the PC_{ox} potential.

With its air-formed film intact, the best behavior observed for 304 stainless steel in anhydrous PC with 0.5 M $LiAsF_6$ is stable passivity up to 4.45 V. However, breakdown and pitting has been observed more frequently at 4.1 to 4.2 V, which is approximately the same potential where breakdown and passivity is observed in technical-grade PC with $LiAsF_6$. Some impurity in anhydrous PC, which is also present in technical-grade PC, is presumably responsible for the behavior. The impurity has yet to be identified.

Current research efforts are seeking to understand the premature breakdown of stainless steel in anhydrous PC and are exploring the passivation/corrosion behavior of the same alloys in another solvent, dimethoxyethane (DME).

PUBLICATIONS

1. R.G. Kelly, P.J. Moran, E. Gileadi, and J. Kruger (1989), "The Passivity of Iron in Mixtures of Propylene Carbonate and Water," *Electrochim. Acta* **34**, 823.
2. R.G. Kelly, P.J. Moran, J. Kruger, C. Zollman, and E. Gileadi (1989), "Passivity of Fe in Anhydrous Propylene Carbonate," *J. Electrochem. Soc.* **136**, 3262.

E. COMPONENTS FOR AMBIENT-TEMPERATURE NONAQUEOUS CELLS

Metal/electrolyte combinations that improve the rechargeability of ambient-temperature nonaqueous cells are under investigation.

Spectroscopic Studies of the Passive Film on Alkali and Alkaline Earth Metals in Nonaqueous Solvents: A Surface Science Approach

D.A. Scherson (Case Western Reserve University)

The main focus of this research project is to elucidate the structure of passive films that form on alkali and alkaline earth metals in nonaqueous solvents. During 1989, investigation of the reactivity of metallic Li towards common organic solvents continued. The approach being utilized involves the vapor deposition of Li onto a host metal surface in ultra-high vacuum, followed by the exposure of such surfaces to nonaqueous solvents in the gas phase. The nature of the reaction products is investigated by Auger electron (AES), X-ray photoelectron (XPS), thermal desorption (TDS), and Fourier transform infrared reflection-absorption (FTIRRAS) spectroscopies. A careful analysis of the results is expected to provide much needed information regarding the nature of the passive film that forms at the nonaqueous solvent-Li interface, which has direct relevance to the shelf life, cycle life, and performance of secondary Li-based batteries.

The construction of the FTIR/UHV chamber in which some of the proposed measurements will be carried out has been completed. Unlike the original approach developed during this past year, which relied both on elliptical and spherical mirrors external to the chamber to direct the IR beam to the sample and later into the detector, the new design uses only flat mirrors placed inside the chamber in order to accomplish the same goal. In this fashion, it has been possible to achieve incident angles >70° with respect to the axis normal to the surface of the sample and at the same time increase considerably the outgoing-to-incoming light intensity ratio.

The feasibility of the proposed FTIR/UHV experiments has been demonstrated using the reaction of CO_2 on vapor-deposited Li as a model system. For these measurements, the UHV chamber was placed on a small table which seats directly on the bottom of the optical bench. This table has a set of screws that allows fine adjustment of the position of the chamber so as to achieve maximum radiation throughput at the desired incident angle. A set of Al plates and compression O-rings enable full isolation of the sample compartment of the FTIR from the atmosphere. This makes it possible to evacuate the spectrometer cavity to a pressure low enough to make the spectral contributions of CO_2 and water vapor undetectable.

Normalized p-polarized spectra were acquired after exposure of a thick layer of vapor-deposited Li on a freshly evaporated Au surface to a partial pressure of CO_2 of 2×10^{-7} torr for about one minute (~10 Langmuirs). The background pressure in the chamber during data collection was about 6×10^{-8} torr. Two hundred interferometric scans were acquired and co-added every seven minutes at a rate of 2 scans per second. An analysis of the spectral data using the spectrum collected after Li deposition, but prior to admitting CO_2 in the chamber as a reference, provided evidence for the presence of a prominent band at about 1450 cm^{-1} that shifts towards higher energies as the time of exposure is increased. This band is characteristic of carbonate that is formed upon the reaction of CO_2 with Li. No further increases in the height of this peak were observed after about 30 min. indicating that all the Li had reacted with CO_2 and that CO_2 did not exhibit any affinity for the reacted carbonate layer.

To gain further insight into the nature of the Li/nonaqueous-solvent passive film, and to draw parallels between the UHV and electrochemical environments, the aforementioned studies will be complemented by *in situ* measurements involving the same type of alkali metal and nonaqueous solvent systems. To increase the sensitivity of the cell, the flat optical window of the spectroelectrochemical IR cell currently in use in this laboratory has been replaced by a dove prism. The performance of this new *in situ* cell design has been examined using a species which was irreversibly adsorbed on Au as a probe, and excellent results were obtained.

In Situ Raman Spectroscopy of the Zinc Electrode Surfaces in Alkaline Solutions Cells

H. Tachikawa (Jackson State University)

The objective of this project is to investigate the nature of the passive film formed on Zn electrode surfaces in alkaline solutions by *in situ* Raman spectroscopy. Zinc electrodes in 7.0 M KOH solutions, with and without saturated ZnO (0.5 M), were studied. Numerous low-intensity bands were observed between 175 and 1700 cm^{-1} when ZnO was not added to the KOH solution. Raman spectra were recorded between 255 and 1700 cm^{-1} with KOH solutions containing ZnO because the high scattering level from the rough electrode surface created problems for observing low frequency bands. Spectra were also recorded in the high wave-number region (2400-3800 cm^{-1}) where OH^- vibrations exist. Raman spectra were recorded at the deposition potential (-1.6 V *vs* Hg/HgO in 7.0 M KOH) and the passivation potentials (–1.1 and –0.7 V). The spectra recorded in ZnO-saturated 7.0 M KOH at –0.7 V, where the formation of a passive film was expected, showed two bands at 391 and 470 cm^{-1} in the 100 to 750 cm^{-1} region. These two bands were also observed at –1.1 V, but the 391 cm^{-1} band disappeared at -1.6 V. The 470-cm^{-1} band has previously been assigned (1) as a V_1 vibrational mode of $Zn(OH)_4^{2-}$. For the assignment of the Raman bands from the surface layer, Raman spectra of both ZnO and Zn(OH) samples were recorded. The strongest Raman band was observed at 437 cm^{-1} which is assigned to ZnO. Other bands were observed at 330, 379, 410, 584, and 1154 cm^{-1}. Of the many Raman bands for $Zn(OH)_2$, a band at 367 cm^{-1} with a shoulder at 380 cm^{-1} showed the strongest intensity.

The observation of a 391 cm^{-1} band from the Zn surface layer at the passivation potential suggests the formation of $Zn(OH)_2$. The Raman spectra which were recorded after applying the anodic polarization potential (-0.80 V) for two hours showed several bands at 332, 390, 448, 480, and 564 cm^{-1}. The presence of both the 332 and 448 cm^{-1} bands may suggest the formation of ZnO at the surface of the Zn electrode (2). The 390 cm^{-1} band indicates the presence of

$Zn(OH)_2$ on the surface of the Zn electrode as well. These results suggest the possible formation of both ZnO and $Zn(OH)_2$ on the Zn electrode when the passive potential is applied for two hours.

In summary, the passive film, which was formed on the Zn surface during the initial film formation process, consisted of $Zn(OH)_2$. Some of the $Zn(OH)_2$ may be transformed to ZnO when the potential of the Zn electrode is kept at the passive potential for a long period of time.

REFERENCES

1. A.G. Briggs, N.A. Hampson and A. Marshall (1974), *J. Chem. Soc. (Faraday Trans II)*, 1978.
2. A.H.L. Goff, S. Joiret, B. Saidani, and R. Wiart (1989), *J. Electroanal. Chem.* **263**, 127.

Polymeric Electrolytes for Ambient-Temperature Batteries

G.C. Farrington (University of Pennsylvania)

The objective of this program is to investigate the chemical and electrochemical characteristics of polymeric electrolytes for use in high-specific-energy batteries. The main focus of research this year was to study and characterize the electrochemical behavior of a new polymer electrolyte with a Li^+ conductivity at room temperature which is comparable to that of nonaqueous liquid electrolytes. This material was developed at the Energy Research Laboratory in Svendborg, Denmark, where researchers are using it as an electrolyte for high-specific-energy batteries (Li/V_6O_{13}). Collaborative work at the University of Pennsylvania involves the study of the electrochemical characteristics of Li oxidation and reduction in this electrolyte system, materials characterization, and a study of the factors that influence Li electrode cycle life. This material is particularly interesting since it appears to have the highest room-temperature Li-ion conductivity yet observed with a polymer electrolyte. In addition, work is currently underway to develop the appropriate facilities at the University of Pennsylvania for the synthesis of these electrolytes. All of the equipment required for this work should be in place by May 1990.

Differential scanning calorimetry (DSC) of the polymer electrolyte containing $LiAsF_6$ as the conductivity salt have shown that the electrolyte is completely amorphous from –90 to 200°C. No evidence of a T_g or of the existence of any crystalline phase was observed. The results from thermal gravimetric analysis (TGA) results show that the electrolyte loses weight slowly between 40 and 100°C (heating rate of 5°C/min) and more rapidly between 100 and 160°C; by 160°C the total weight loss is about 30%.

Reversible and reproducible cyclic voltammograms of a symmetric cell of the type, Li/Li^+/polymer electrolyte/Li (at room temperature), were obtained by scanning between ±2.5 V at a rate of 5 mV/sec. Increasing the scan rate increases the overall current as expected. Under optimum conditions the oxidation/reduction process seems quite reversible. When multiple sweep are carried out, the peak position and peak current do not change appreciably after the first cycle. Some of the cells could be cycled 25-30 times before shorting occurred.

The new polymer electrolyte appears to be quite promising for application in ambient-temperature Li cells. Further studies already underway will characterize its electrochemical characteristics in more detail.

Exploratory Cell Research and Fundamental Process Study in Solid-State Electrochemical Cells

W.H. Smyrl (University of Minnesota)

The objectives of this program are to perform research to support the development of high-performance rechargeable batteries that are desired for electric vehicles or utility load-leveling systems. The major thrust was to investigate solid-polymer-electrolyte rechargeable cells based on poly(ethylene oxide) (PEO) using Na and divalent metal anodes that are alternatives to Li. Other studies were also conducted with poly(pyrrole) (PPY) for the cathode. Sodium/solid polymer electrolyte rechargeable cells of the type $Na/NaCF_3SO_3(PEO)_8/V_6O_{13}$ and $Na/NaCF_3SO_3(PEO)_8/PPY$ were investigated. This project was completed in 1989.

Differential scanning calorimetry (DSC) and x-ray diffraction studies were conducted on $(NaCF_3SO_3)_xPEO$. These studies showed that when $x < 0.2$, two phases exist at room temperature — a crystalline PEO phase and a crystalline intermediate compound. At $x > 0.2$, only the crystalline intermediate compound is observed. At temperatures >60°C a mixed phase is present for $x < 0.2$ which has a higher conductivity than the crystalline phase or that of the intermediate compound. The high conductivity is attributed to the presence of a liquid phase, which permits the rapid transport of Na^+ ions.

Poly(pyrrole) (PPY) was found to be stable in aqueous and oxygen environments. Its disadvantages

are: *i)* reversible doping (oxidation) is limited to about 30%, and *ii)* the large changes in conductivity between the oxidized (high conductivity) and reduced (low conductivity) states. A $Na/NaCF_3SO_3(PEO)_8/PPY$ cell was fabricated using thin-film technology. The cell had an open-circuit voltage of 2.45 V at 100°C and a theoretical capacity of 22.7 μAh. The cell was discharged at a constant current of 7.6 μA (C/3 rate) to a cell voltage of 1.5 V, and charged at constant current of 7.6 μA to 3.1 V. The observed capacity was 45% of theoretical, and the coulombic efficiency was 70% for the first cycle. The subsequent four cycles also showed a similar performance. This project has been completed.

PUBLICATIONS

1. M. Lien and W.H. Smyrl (1989), "Impedance Analysis of Poly(vinylferrocene) Films Spin-Coated on Metal Substrates," in *Proc. of the Symposium on Transient Techniques in Corrosion Science and Engineering*, W.H. Smyrl, D.D. Macdonald and W.J. Lorenz, eds., The Electrochemical Society, Inc., Pennington, NJ, p. 286.
2. W.H. Smyrl and C.H. Paik (1989), "Impedance Characterization of Electrochemistry of Conducting Polymers," in *Proc. of the Symposium on Transient Techniques in Corrosion Science and Engineering*, W.H. Smyrl, D.D. Macdonald and W.J. Lorenz, eds., The Electrochemical Society, Inc., Pennington, NJ, p. 270.
3. M.Z.A. Munshi, A. Gilmour, W.H. Smyrl and B.B. Owens (1989), *J. Electrochem. Soc.* **136**, 1847.

Solid Polymer Electrolytes for Rechargeable Batteries

D. Macdonald and S. Narang, SRI International

The objective of this research is to develop advanced ion-conducting polymers that can be used as solid polymer electrolytes (SPE) in high-specific-energy rechargeable batteries. Batteries of this type (*e.g.*, $Li/SPE/TiS_2$, $Li/SPE/LiNi_{1-x}Co_xO_2$) have the potential for virtually maintenance-free reliable operation over hundreds of cycles. SPE-based batteries should have lower cost of fabrication, longer shelf life, longer cycle life, and no electrolyte leakage. The polymer of interest in this research are polyethyleneimine-based SPEs.

Poly(ethyleneimine) derivatives containing oligoether side groups,

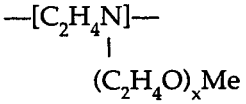

where x = 3 (*i*), 4 (*ii*), and 8.23 (*iii*) have been prepared from linear poly(ethyleneimine) in a two-step reaction sequence. Salt complexes for these polymers *(i-iii)* were prepared by dissolving stoichiometric quantities of $LiCF_3SO_3$ in a common solvent and drying under vacuum.

The log σ *vs* 1/T plot indicates a behavior explicable by free-volume-theory, and ion-transport is promoted by polymer segment motion. The optimum concentration of $LiCF_3SO_3$ required for polymers *ii* and *iii* has been found to be 16 ether oxygens per Li^+ ion; if the concentration of $LiCF_3SO_3$ increases or decreases, the ambient-temperature conductivity decreases. However, salt complexes formed by polymer *i* show very low conductivity. This result suggests that the side groups should contain at least four ether oxygens to obtain appreciable conductivity. Moreover the conductivity of salt complex formed by

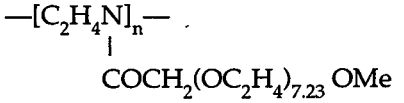

is ~10 times lower than that of polymer *iii* since the presence of amide group restricts the freedom of rotation around the nitrogen atom. It can be seen that the conductivity of these complexes (highest conductivity is 3.3×10^{-6} ohm^{-1}-cm^{-1} at 22°C) are comparable to salt complexes formed by poly(phosphazene) or poly(siloxane) derivatives.

Having established that the poly(ethyleneimine) derivatives exhibit high conductivity with $LiCF_3SO_3$, single-ion conducting polymers with oligoether and fluorosulfonates as pendant groups have been prepared in a three-step reaction sequence from linear poly(ethyleneimine). The following polymers,

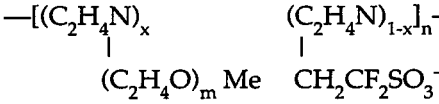

where (1) m = 4, x = 0.61 and 0.66, M = Na^+, and (2) m = 8.23, x = 0.61, 0.66, 0.81 and 0.93, M = Li^+ or Na^+, have been prepared and characterized. Sodium- and lithium-ion conductivities have been measured by ac impedance spectroscopy. Among the compositions investigated for these polyelectrolytes, the trend in conductivity for Na^+ and Li^+ ions is opposite to each other. This observation agrees with the effective ionic radii and the lattice energies of these ions. The high-

est Li-ion conductivity is found to be 1.7×10^{-7} ohm^{-1}-cm^{-1} at 40°C. Although this is very low for practical use in a battery, the conductivity was increased to 4×10^{-5} ohm^{-1}-cm^{-1} at ambient temperature when the polymer film was exposed to acetonitrile (AN) vapors. The AN acts like a plasticizer and opens up the polymer chains to allow the Li ions to move more freely.

F. CROSS-CUTTING RESEARCH

Cross-cutting research is carried out to address fundamental problems in electrocatalysis, current-density distribution and gas evolution, solution of which will lead to improved electrode structures and performance in batteries and fuel cells.

Analysis and Simulation of Electrochemical Systems

J.S. Newman (Lawrence Berkeley Laboratory)

This objectives of this project are to *i*) investigate efficient and economical methods for electrical-energy conversion and storage, *ii*) develop mathematical models to predict the behavior of electrochemical systems and identify important process parameters, and *iii*) verify experimentally the completeness and accuracy of the models. Recent activities have focused on the following areas: *i*) investigations of the formation of salt films on electrochemically active surfaces, *ii*) fundamental studies of the electroprecipitation method for producing Ni electrodes for high-energy batteries, *iii*) alternating-current analysis of porous electrodes, *iv*) alternating-voltage measurements on the dissolution of Cu and Zn, *v*) development of boundary-integral techniques for the numerical solution of current and potential distribution problems, *vi*) mathematical modeling of transport processes in solid-polymer electrolytes, *vii*) studies of self-generated magneti fields in high-power batteries, and *viii*) determination of transport properties in sodium polysulfide melts.

The mathematical model of the electrochemical oscillations in the corrosion of Fe in sulfuric acid, which includes a porous ferrous sulfate film, was modified to account for the kinetics of salt-film dissolution. The kinetics of the dissolution and precipitation of porous ferrous sulfate films was investigated with rotating ring-disk electrodes (RRDE). The investigation explained some of the complex behavior observed when Fe dissolves in sulfuric acid. This experimental approach should be applicable to other porous salt films. The concentrated-solution model will be extended to include a porous film on the electrode surface. The rate of dissolution of ferrous sulfate films in 1 M H_2SO_4 was investigated with a RRDE system at two temperatures. Results indicate that the nonelectrochemical dissolution of salt films is usually mass-transfer limited. Consequently, the modeling of electrochemical systems containing porous salt films, whether they be part of a battery or corrosion system, is simplified, for it is unnecessary to choose a kinetic rate constant for this reaction.

Mass transfer to a rotating-disk electrode (RDE) in dilute, electrolytic solutions with a reacting supporting electrolyte has been studied. The effect of finite rates of homogeneous complexing reactions was studied using a perturbation analysis. The model predicted potential and concentration variations and impedances.

A model has been developed to predict the response of a redox reaction with soluble reactants and products in a flow-through porous electrode to alternating currents. The model accounts for double-layer capacity.

A model for simulating cyclic voltammetry has been modified to account for adsorption of chemical species on the electrode, the chemical or electrochemical reaction of the adsorbed species, and convective diffusion to a RDE. The simulation of the nitrate reduction reaction will be used as an aid to study the electroprecipitation of nickel hydroxide.

A general analysis, using singular perturbations and boundary-integral techniques, has shown the distribution of current density near the edge region of an insulator and electrode for fast, but finite, kinetics. The analysis has been carried out for linear and Tafel kinetics, and it should provide a valuable tool for the verification of other numerical analyses. Additionally, under certain conditions the analysis can predict completely the distribution of current density without any further numerical calculations.

A one-dimensional mathematical model of transport in conducting polymers has been developed. This model has been applied to the perfluorinated ionomer separator in a solid-polymer-electrolyte fuel cell. Transport properties were estimated as a function of water content, and water-management in the separator of a solid-polymer fuel cell was examined.

The current distribution in a one-dimensional geometry, chosen to approximate that of a bipolar, high-power battery, has been determined. This simple model, based on Maxwell's electrodynamic equations, has provided an estimate of the inductance of the battery as well as the profiles of current in the electrodes.

A mathematical model of the $Na/FeCl_2$ battery containing a molten $AlCl_3$-NaCl electrolyte cell was developed. The effects of the state of discharge, the cell temperature, the precipitation and dissolution rates of NaCl, and the current density on the current-potential relationship during charging and discharging cycles, were examined.

PUBLICATIONS

1. A.C. West and J. Newman (1989), "Corrections to Kinetic Measurements Taken on a Disk Electrode," *J. Electrochem. Soc.* **136**, 139. LBL-24416.
2. W.H. Smyrl and J. Newman (1989), "Current Distribution at Electrode Edges at High Current Densities," *J. Electrochem. Soc.* **136**, 132. LBL-23905.
3. A.K. Hauser and J. Newman (1989), "Singular Perturbation Analysis of the Faradaic Impedance of Copper Dissolution Accounting for the Effects of Finite Rates of a Homogeneous Reaction," *J. Electrochem. Soc.* **136**, 2820. LBL-25706.
4. A.K. Hauser and J. Newman (1989), "The Effect of Schmidt Number on the Faradaic Impedance of the Dissolution of a Copper Rotating Disk," *J. Electrochem. Soc.* **136**, 2896. LBL-25721.
5. A.C. West and J. Newman (1989), "Current Distribution near an Electrode Edge as a Primary Distribution is Approached," *J. Electrochem. Soc.* **136**, 2935. LBL-26153.
6. A.K. Hauser and J. Newman (1989), "Effects of Finite Rates of a Homogeneous Reaction on the Steady-State Dissolution of Copper in Chloride Solutions," *J. Electrochem. Soc.* **136**, 3249. LBL-25584.
7. A.K. Hauser and J. Newman (1989), "Potential and Concentration Variations of a Reacting, Supporting Electrolyte," *J. Electrochem. Soc.* **136**, 3319. LBL-25608.
8. S. Thompson and J. Newman (1989), "Differential Diffusions Coefficients of Sodium Polysulfide Melts," *J. Electrochem. Soc.* **136**, 3362. LBL-23820.
9. A.C. West and J. Newman (1989), "Interpretation of Kinetic Rate Data Taken in a Channel Flow Cell," *J. Electrochem. Soc.* **136**, 3755. LBL-26621.
10. A.K. Hauser and J. Newman (1989), "Application of the Macroscopic and Microscopic Impedance Models to the Analysis of the Total Electrochemical Impedance of Copper Dissolution," LBL-26269.
11. A.K. Hauser and J. Newman (1989), "A Macroscopic-Impedance Model for a Rotating Disk-Electrode," LBL-26267.
12. A.K. Hauser and J. Newman (1989), "A Microscopic-Impedance Model for a Rotating-Disk Electrode," LBL-26268.
13. M. Sudoh and J. Newman (1989), "Mathematical Modeling of the Sodium/Iron Chloride Battery," LBL-26896.
14. A.C. West, J.H. Sukamto, and J. Newman (1989), "A Criterion to Verify Current Distribution Calculations," LBL-27474.
15. A.C. West and J. Newman (1989), "Current Distribution on Recessed Electrodes," LBL-28045.
16. A.A. Mason and J. Newman (1989), "Optimization of the $LiAl/FeS_x$ Molten-Salt Batteries," LBL-26630.
17. A.K. Hauser (1989), Ph.D. Thesis, "Steady-State and Impedance Analyses of Electrochemical Kinetics and Mass Transfer," LBL-27123.
18. A.C. West (1989), Ph.D. Thesis, "Effects of Nonuniform Current and Potential Distributions in Electrochemical Systems," LBL-28076.
19. T.F. Fuller and J. Newman (1989), "A Concentrated Solution Theory Model of Transport in Solid-Polymer-Electrolyte Fuel Cells," in *Proc. of the Symposium on Fuel Cells*, Volume 89-14, R.E. White and A.J. Appleby, eds. The Electrochemical Society, Inc., Pennington N.J., p.25.

Surface Layers on Battery Materials

R.H. Muller (Lawrence Berkeley Laboratory)

The purpose of this work is to advance the understanding of properties of surface layers on battery electrode materials that are important for the functioning of rechargeable galvanic cells with high specific energy and power capabilities, energy efficiency, charge retention, and cycle life. Means are sought to achieve superior, predictable properties of surface layers and to form them consistently to provide enhanced battery operation. Present studies are concerned with oxide formation on different metals and the cathodic deposition of Zn from alkaline media.

Oxidation films that form on battery materials are often composed of semiconducting oxides and insulating hydroxide phases. Laser Raman spectroscopy was used to investigate the semiconducting oxides of Zn, Cu, and Ni that form during anodization in alkaline media. The possible interaction of the high-intensity laser probe beam with the surface to modify interfacial electrochemical processes during *in situ* Raman studies was studied. Cyclic voltammograms of a Cu electrode in 1 M KOH have been found to be

different whether the electrode is observed in the dark or under illumination by a focused laser beam (514 nm, 1000 W/cm^2). The reduction of oxide layers is facilitated by illumination. Modulation of the illumination at 50 Hz and measurement of the in-phase cathodic photo-current produced reduction peaks at –50 and –400 mV (*vs* Hg/HgO). Raman spectroscopy showed the formation of Cu_2O (from bivalent layers such as CuO) at –50 mV and reduction of the p-type Cu_2O to metal near 400 mV.

A comparison of elastic light scattering measurements during the galvanostatic formation of Ag_2O in KOH with predictions based on an optical model with a random 2-dimensional array of spherical particles of equal radius has shown that the observed angular distribution can be fitted in the early stages of film formation by adjusting particle size and number density, although unrealistically large particle sizes have to be assumed (150-220 nm). At the later stages of growth, the fit becomes progressively worse. It appears that the model is at best an approximate representation of the oxide film, and its assumptions are not valid after redistribution of the film material. Scattering measurements have therefore been interpreted by two global quantities, the root mean square (RMS) roughness, derived from the integral of the spectral power density function, and the near-to-far-angle spectral power density ratio. The ratio is a measure of particle size.

Studies on structural changes in nickel oxide films, as a possible cause for the memory effect of Ni electrodes in galvanic cells, have concentrated on the reproducible preparation of metal and oxide surfaces and the determination of their spectral optical constants. One-dimensional, two-film optical models have been shown not to be adequate to represent the transformations between nickel hydroxide and oxyhydroxide.

The multilayer electrodeposition of Pb on polycrystalline Ag was studied by *in situ* scanning tunneling microscopy (STM). Film growth was found to involve a series of alternating roughening and smoothing stages. Surface topographies were characterized quantitatively by the calculation of amplitude density and autocorrelation functions from the STM images. The observations have been interpreted in terms of the repeated nucleation at thermodynamically favored recessed areas of the surface.

Mass transfer to a small-aspect-ratio rotating disk chemical vapor deposition (CVD) reactor has been analyzed theoretically. With the use of a porous injector facing the rotating disk, this system can provide uniform reaction rates over most of the surface of the disk. Perturbation expansions for the concentration field and deposition rate induced by a mass-transfer limited reaction on the rotating disk have been prepared. The perturbation solutions for the effect of injection velocity, substrate rotation rate, and fluid properties compare well with numerical solutions in the literature.

PUBLICATIONS

1. R.H. Muller (1989), "Microtopography of Electrochemical Surface Layers," *40th Meeting of the International Society of Electrochemistry*, Kyoto, Japan, Abstract No. 19-05-04. LBL-26742.
2. D.T. Schwartz and R.H. Muller (1989), "Mass Transfer in a Small Aspect Ratio Rotating Disk CVD Reactor," LBL-27882.
3. S.T. Mayer (1989), *Ph.D. Thesis*, "An *In Situ* Study of the Anodic Film Formation of Cu, Ag and Zn in Alkaline Media," LBL-28085.

Application of Photothermal Deflection Spectroscopy to Electrochemical Interfaces

E.J. Cairns and F.R. McLarnon (Lawrence Berkeley Laboratory)

Photothermal deflection spectroscopy (PDS) is being used to study reactions at electrochemical interfaces. PDS is a sensitive *in situ* technique that measures the absorption spectrum of an electrochemical interface. This information helps to identify the reaction intermediates, which in turn help to determine the pathway by which the reaction occurs. PDS also measures the electrolyte concentration gradients adjacent to the electrode surface. These gradients contain information about the diffusion of reactants and products to and from the electrode. The sensitivity of these measurements is high enough to detect reactions involving a single molecular layer of species on the electrode surface. Mathematical models of the chemical and physical processes occurring at the electrode surface have been developed. These models allow the complex interaction of parameters governing the PDS system to be analyzed. These models have resulted in a more-quantitative understanding of the PDS system. A method of measuring infrared absorption spectra has been developed. The major difficulty with prior optical investigations using this region of the spectrum is that many electrochemical systems of

interest use water-based electrolytes that are nearly opaque in the infrared. Aided by mathematical models, a new cell has been designed that uses only a thin layer of electrolyte. This cell allows the PDS system to obtain infrared spectra, and preliminary experiments have been successful. Future experiments will measure the spectrum of the species on Pt electrodes during the electrooxidation of CH_3OH.

Fuel cells based on the direct electrooxidation of methanol promise an efficient, environmentally sound, alternative power source for vehicles. Unfortunately, the anodic reaction on Pt electrodes exhibits a large overpotential due to poorly understood poisoning reactions, rendering the above application economically unattractive. A significant enhancement of the reaction rate has been observed on Pt-Ru alloy electrodes, and the quantitative characterization of this enhancement is the subject of this research. An all-Teflon cell was designed and is being built, which permits an assessment of the rate of CH_3OH electrooxidation in HF and H_2SO_4 electrolytes at temperatures up to 100°C. Indications of preferential dissolution of Ru from these electrodes suggest that an investigation of the alloy's surface *vs* bulk composition should be carried out in order to guarantee meaningful comparisons of catalyst (electrode) activities; AES will assist in doing so. In addition, the evaluation of the real catalyst surface area will be an important task, which is not as easily carried out on Pt-Ru as it is on Pt alone. The PDS in combination with the above electrochemical evaluations are being used to elucidate the mechanisms of CH_3OH electrooxidation reactions, thereby providing a means for the "intelligent" design of more-efficient catalysts.

PUBLICATIONS

1. J.D. Rudnicki, F.R. McLarnon, and E.J. Cairns (1989), "*In Situ* Characterization of Electrode Processes by Photothermal Deflection Spectroscopy," in *Techniques for Characterization of Electrodes and Electrochemical Processes*, R. Varma and J.R. Selman, eds., The Electrochemical Society, Pennington, NJ, and John Wiley and Sons, NY. LBL-27081.
2. J.D. Rudnicki, R.E. Russo, F.R. McLarnon, and E.J. Cairns (1989), "Photothermal Deflection Spectroscopy: An *In Situ* Technique for the Investigation of Electrochemical Interfaces," *175th Meeting of the Electrochemical Society*, Los Angeles, CA, Abstract No. 543. LBL-26726.

Electrode Kinetics and Electrocatalysis of Methanol Electro-oxidation

P.N. Ross (Lawrence Berkeley Laboratory)

The objective of this research is to investigate the direct oxidation of methanol on modified Pt electrocatalysts. This study uses modern surface analytical methods, [*e.g.*, LEED, AES, XPS, ion-scattering spectroscopy (ISS)], coupled with electrochemical methods to determine the dependence of catalytic activity on the composition and structure of modified Pt surfaces.

A study of the electrochemistry of Pt_3Sn was completed. Even though this alloy has a very exothermic heat of mixing, surface enrichment of Sn occurs on all three low-index faces, (111), (100), and (110). The (110) surface actually reconstructs in the first few atomic layers to a distorted form of the hexagonal structure of the ordered stoichiometric alloy PtSn. The surface composition of all three faces appears to be 50% Sn, *vs* 25% in the bulk. Neither methanol nor CO is adsorbed from the gas phase onto the Pt_3Sn surface at room temperature. The voltammetry indicated that there was no hydrogen adsorption on the Pt_3Sn surface in acid electrolyte, and the surface was a very poor catalyst for methanol oxidation. Two properties of this material appear to be causing the low activity: *i)* strong intermetallic bonding reduces the number of Pt d-electrons available for bonding to adsorbates, and *ii)* the concentration of Sn in the surface is too high, and a critical ensemble of Pt-Pt sites may be required for effective catalysis.

The study of Pt surfaces modified by electrodeposited Sn is still in progress. On a polycrystalline Pt sample, a 50-fold acceleration of the rate of methanol oxidation in sulfuric acid was observed, but much smaller effects were observed on the low-index single-crystal surfaces. Thus, there appears to be a very surprising effect of the surface structure on the catalytic effect, possibly a different state of Sn results from adsorption on the different Pt faces.

PUBLICATIONS

1. A. Norton-Haner and P.N. Ross (1989), "Surface Chemistry of Single Crystal Pt_3Sn," LBL-28074.
2. A. Norton-Haner and P.N. Ross (1989), "Electrocatalytic Oxidation of Methanol on Sn Modified Pt Surfaces: The Alloy versus the Adatom State," LBL-28399.

Engineering Analysis of Gas Evolution

C.W. Tobias (Lawrence Berkeley Laboratory)

The objective of this project is to elucidate the role of free and forced convection as it affects overpotential behavior and ohmic resistance in electrolytic gas evolution processes, and to clarify the effect of concurrent gas evolution on surface morphology in metal deposition processes. Gas coverage and detachment, as well as behavior in suspension, is observed by normal- and high-speed cinematography. The channel flow cell constructed for this purpose incorporates an easily changeable, coplanar square 1 x 1 cm electrode surface, which is illuminated by fiber optics to achieve sufficiently high intensity of illumination. The counter-electrode is situated in the walls normal to the electrode that is observed. Electrode overpotential is continuously monitored.

Coalescence phenomena between similar (H_2–H_2) or different (H_2–O_2) gas bubbles are observed on precisely aligned microelectrodes facing each other. Spherical bubbles may be evolved at suitably low rates, until they touch and the actual coalescence event occurs. Supersaturation at H_2- or O_2-evolving electrodes is measured by electrochemical techniques and is correlated to surface coverage and bubble frequency.

Ten-by-ten quadratic planar matrices of square Pt surface elements with 100-μm edge length, electrically isolated from each other, serve as models to simulate polycrystalline surfaces. Matrices were manufactured on silicon wafers by Hewlett-Packard Company and Bell Laboratories. These unique devices facilitate the nucleation, growth, and coalescence of bubbles at predetermined locations, and the simultaneous monitoring of electrode potentials. A data-acquisition system, designed and built in-house, and a program also developed in-house, monitors current to each of 100 segments and controls the growth of bubbles.

A surface renewal model has been developed to predict hydrogen supersaturation levels over horizontal electrodes. While excellent agreement was obtained with experimental data for platinized electrodes, further measurements of surface coverage are deemed necessary to determine model parameters for polished surfaces.

The effect of parallel streams of bubbles rising along a vertical electrode surface on mass transfer and supersaturation was investigated. Previous work in this laboratory has successfully predicted the increased limiting current to the surface in the vicinity of a rising single stream of bubbles. The analysis modeled the stream as a moving cylinder. A curtain of bubbles approximates actual behavior more closely during gas evolution. The micromosaic electrode developed in this laboratory has been redesigned to include satellite pads that may be used as "bubble-generating segments." The original set of electrodes fabricated by Hewlett-Packard suffered rapid corrosion of the Cr underlying the Pt surface elements; they had a maximum effective lifetime of six hours in the aggressive sulfuric acid solutions used in H_2 evolution experiments. In the modified manufacturing technique, the Cr layer has been replaced by Ticusil (a corrosion resistant alloy) and Ti, which is corrosion resistant as well. The instrumentation required for the operation of the micromosaic device has been updated; data can now be acquired through a pair of 16-bit i/o boards connected to an IBM-AT clone, improving both the speed and quantity of data acquisition.

IV. AIR SYSTEMS RESEARCH

The objectives of this project element are to identify, characterize, and improve materials for air electrodes; and to identify, evaluate, and initiate development of metal/air battery systems and fuel-cell technology for transportation applications.

A. METAL/AIR CELL RESEARCH

Projects on metal/air cell research address O_2 electrocatalysis; bifunctional air electrodes, which are needed for electrically rechargeable metal/air (Zn/air, Fe/air) cells; and novel alkaline Zn electrode structures, which could be used in either electrically recharged or mechanically recharged cell configurations.

Electrocatalysts for Oxygen Electrodes

E. Yeager (Case Western Reserve University)

The overall objective of this research is to develop more-effective electrocatalysts for O_2 reduction and generation which have high activity and long-term stability. Research was conducted on various electrocatalysts including the transition-metal macrocycles and oxide catalysts, and was used to identify stable catalysts with much higher activity, for both monofunctional and bifunctional air electrodes. The research accomplishments during 1989 follow.

Transition-Metal Macrocycle Catalysts. Earlier *in situ* studies of the adsorbed transition-metal phthalocyanines (tetrasulfonated phthalocyanines and tetrapyridino porphyrazines) on Ag, using surface-enhanced Raman scattering and resonance Raman together with linear sweep voltammetry, have generally provided evidence for the edge-on configuration with the plane of the ligand perpendicular to the surface. The *in situ* UV-visible reflection-absorption studies have also supported this configuration.

During the past year, *in situ* FTIR measurements have been carried out with a monolayer of adsorbed FeTsPc on Ag and ordinary pyrolytic graphite (OPG) using the subtractively normalized interfacial FTIR (SNIFTIRS) technique. A specially developed thin-layer infrared reflection/absorption cell has been used for this study. This cell normally affords sufficient sensitivity to observe the major peaks for the adsorbed monolayer and the corresponding solution phase organic species in the thin layer of the electrolyte. It is generally possible to distinguish adsorbed species from the solution-phase species in this thin-layer cell because the peaks in the spectra are shifted relative to those of the solution-phase and would have a significant dependence on potential (Stark effect). In the present studies, the macrocycle was preadsorbed on the electrode surface under conditions where a monolayer formation is expected.

Only some of the peaks associated with the sulfonate species were observed. None of the modes expected for the pyrrole and aromatic were seen. This may be explained in terms of the perpendicular orientation on the basis that only sulfonic acid groups experience the high field gradient at the interface and only these frequencies are shifted and hence detected. An alternate explanation is that the molecule lies flat and the measurements respond only to modes with a permanent dipole perpendicular to the surface. These modes would be relatively low frequencies and probably relatively weak, thus making them difficult to detect. The sulfonic acid groups would have components perpendicular to the surface and afford much greater sensitivity. The CWRU group favors the first explanation based on the perpendicular orientation but further work is necessary to ensure the proper interpretation of the FTIR studies. Other configurations in which the macrocycle is partially inclined to the surface are also possible.

The recent voltammetric studies indicate a strong dependence of the peak heights and width on the conditions under which the macrocycle is preadsorbed (*i.e.*, potential, electrolyte, and pH). The μ-oxo $(FeTsPc)_2O$ species has also been observed in bulk alkaline solution but not in the FeTsPc layers adsorbed on metal or graphite from either alkaline or acid solutions nor in the solid state.

FeTsPc and CoTsPc adsorbed on Ag increase the catalytic activity for O_2 reduction in alkaline solution (shift the polarization by ~100 mV positive) even though Ag is itself a moderately active catalyst for this reaction.

Ex situ FTIR reflectance studies of cobalt tetramethoxyphenylporphyrin (CoTMPP) adsorbed on highly ordered pyrolytic graphite (HOPG) provide evidence for differences in the orientation of the CoTMPP when the surface film is prepared by different methods.

The addition of axial ligands such as CN– which can bind selectively with the transition metals in specific valency states has provided a powerful tool for confirming which redox couples are important for O_2

electrocatalysis. Research has been initiated in the use of the scanning tunneling microscope (STM) for *in situ* as well as *ex situ* examination of adsorbed transition metal macrocycles on low-index single crystal surfaces (HOPG, Pt, Au). Transmission electron microscopy (*ex situ*) measurements have already been initiated using the JEOL 4000 with 0.14-nm resolution and other high-resolution microscopes in the Materials Science and Engineering Department of CWRU. Special techniques are being developed that should facilitate the study of macrocycles on carbon and graphite substrates including HOPG. With the sheet-type polymer macrocycles we expect to establish whether the polymeric ligands are in linear arrays or two-dimensional arrays.

Polymer-Modified Electrodes. Polyvinyl pyridine (PVP) modified electrodes, containing CoTsPc adsorbed at monolayer coverages on OPG, have significantly higher activity and stability for O_2 reduction in acid electrolytes, although the activity is low compared to that of Pt in dispersed high-area form.

Self-Supported Pyrochlore Electrocatalysts. The pyrochlore $Pb_2Ru_2O_{6.5}$ in self-supported, high-surface-area form has been shown to have high activity for the 4-electron reduction of O_2 in alkaline solution. In gas-fed O_2 cathodes using a pore-former (ammonium bicarbonate), the cathodic performance in KOH is significantly better than achieved with carbon supports. In the anodic mode loss of the pyrochlore into the bulk electrolyte is a problem. The application of an ionomer polymer layer to the solution side of the electrode does improve stability and activity in the anodic mode in KOH.

PUBLICATIONS

1. D. Chu, D. Tryk, D. Gervasio, and E.B. Yeager (1989), "Examination of the Ionomer/Electrode Interface using the Ferric/Ferrous Redox Couple," *J. Electroanal. Chem.* **272**, 277.
2. I. Bae, X. Xing, E.B. Yeager, and D. Scherson (1989), "Ionic Transport Effects in *In-Situ* Fourier Transform Infrared Reflection Absorption Spectroscopy," *Anal. Chem.* **61**, 1164.
3. M.S. Hossain, D. Tryk, and E. Yeager (1989), "The Electrochemistry of Graphite and Modified Graphite Surfaces: The Reduction of O_2," *Electrochim. Acta* **34**, 1733.
4. S. Gupta, D. Tryk, I. Bae, W. Aldred, and E. Yeager (1989), "Heat-Treated Polyacrylonitrile-Based Catalysts for Oxygen Electroreduction," *J. Appl. Electrochem.* **19**, 19.
5. A.A. Tanaka, C. Fierro, D.A. Scherson, and E. Yeager (1989), "O_2 Reduction on Adsorbed Tetrapyridinoporphyrazine," *Materials Chemistry and Physics* **22**, 431.
6. H. Chubao, D. Tryk, and E. Yeager (1989), "Electroreduction of O_2 on Pyrolytic Graphite Electrode with Adsorbed Layer of Cobalt Tetrasulfonated Phthalocyanine in Acetonitrile and Dimethylformamide," *Chem. J. of Chinese Universities* **5**, 164.

Electrical and Electrochemical Behavior of Particulate Electrodes

J.W. Evans (Lawrence Berkeley Laboratory)

The purpose of this research is to investigate the electrochemical behavior of Zn/air cells that utilize particulate Zn electrodes. The Zn (or Zn-coated) particles form a stationary bed, and electrolyte flow through this electrode occurs by natural convection. The cathode is a monofunctional air electrode that is available commercially.

In 1989, it was established that a cell employing a particulate Zn anode and natural convection of the electrolyte had a performance comparable to the Zn/air cell which contained a reticulated flow-through structure for Zn deposition. Since that time the performance of the cell with the particulate electrode has been further tested and improved. Cells with electrode area of 80 cm^2 have been operated at current densities up to 148 mA/cm^2, yielding a maximum power of 105 mW/cm^2 (at 20% depth of discharge). Extrapolating this performance to a 32-kWh battery yields a specific power of 238 W/kg (compared to the DOE electric van specification of 80-130 W/kg) and a specific energy of 177 Wh/kg (compared to the DOE 60-120 Wh/kg specification).

The success of laboratory-scale cells (up to 400 cm^2 in cross-sectional area) employing particulate Zn electrodes mandates an investigation of how such cells may be scaled up to a battery for use in electric vehicles. Scale-up will be facilitated by further experimental investigation, coupled with mathematical modeling of the cell. Research is underway or being planned in the following areas:

i) Analysis of natural convection in a cell with a packed-bed electrode.

ii) Regeneration of the particles (probably in a fluidized bed) by electrodeposition of Zn from spent electrolyte.

iii) Long-term performance of air electrodes and other cell components such as diaphragms on exposure to alkaline zincate solutions.

iv) The effect of various driving cycles on cell performance.

v) Pragmatic questions such as how the spent particles and electrolyte are best removed from the cell and replaced with fresh ones.

vi) The capability of the electrolyte to accommodate the Zn discharge products has proven to be unusually high in laboratory cells; because this is a major parameter in determining the specific power and energy of a Zn/air cell, this phenomenon requires further investigation.

PUBLICATION

1. J.W. Evans and G. Savaskan (1989), "A Zinc-Air Cell Employing a Packed Bed Anode," LBL-28290.

Zinc/Air Battery Development for Electric Vehicles

R.A. Putt (MATSI, INC.)

The initial phase of this program was to extend the development of a novel Zn electrode concept which was invented at LBL. In this concept, a reticulated Cu foam material is used as a substrate on which Zn is deposited during charge. Electrolyte flows through the porous electrode structure to supply Zn ions and permit the use of appropriate hydrodynamics to achieve the desired deposit morphology. This flowing-electrolyte scheme facilitates optimization of electrodeposition on charge, which may then be altered to optimize performance on discharge.

The specific objectives of this project are to: *i*) demonstrate Zn loadings of ≥100 mAh/cm^2, *ii*) demonstrate a cycle life of at least 600 cycles in reticulated electrode structures for Zn/air cells, *iii*) develop a preliminary engineering design for a practical Zn/air cell, and *iv*) conduct a preliminary cost analysis for a Zn/air battery stack.

Laboratory testing of Zn/Zn cells (1.3 Ah Zn capacity) showed that through proper cell design and operation 100 mAh/cm^2 loading can be obtained routinely without dendrite growth or nonuniform deposition. Cycle testing (8-h charge, 8-h discharge) of two Zn/Zn cells are continuing, with 510 cycles on cell #1 and 152 cycles on cell #2 (as of 2/28/90). Exceeding the 500-cycle goal established for preliminary feasibility of electric vehicle batteries is a major achievement of the project, and demonstrates the viability of the reticulated structure for secondary Zn electrodes. A dense Zn preplate on the reticulated Cu substrate was found to prevent the irreversible buildup of a resistive oxide layer during cycling. The cycle tests also showed that the maximum Zn loading should be limited to 120 mAh/cm^2 to avoid dendrite problems which occur at higher loadings. At higher loadings the deposit is nonuniform, with a more-dense deposit at the front face where dendrite growth and edge growth becomes problematic.

A monopolar, plate-and-frame construction was designed for the cell stack. An injection-molded plastic frame to retain the Zn electrodes, as well as to provide electrolyte flow and current collection to an external bus bar, is proposed. The O_2 electrode assembly permits two electrodes to be positioned back-to-back against another molded frame, which provides air access to the back sides of the electrode. The assemblies for the Zn and O_2 electrodes are interleaved with separators and gaskets, and the complete cells are held together by two end plates. This monopolar design was judged to be superior to a bipolar design, based on its lower cost and higher energy efficiency. In addition, the monopolar cell design does not require a bipolar separator which is susceptible to corrosion in a bipolar stack design.

A preliminary analysis indicated a cost estimate that ranged from $51/kWh to $71/kWh for the cell stack components. The stack cost is dominated by the cost of the Zn electrode substrate (reticulated structure) and the Celgard separator (*i.e.*, estimated to be >50% of component cost). Including the balance-of-system, the total battery cost is projected to be under $100/kWh.

B. FUEL CELL RESEARCH

Fuel cell research includes projects in several areas of electrochemistry: theoretical studies, fuel-cell testing, fuel processing, and fuel-cell component characterization.

Fuel Cells For Renewable Applications

S. Gottesfeld (Los Alamos National Laboratory)

The primary focus of the Fuel Cell Program at LANL is on the development of polymer-electrolyte-membrane (PEM) fuel cells for transportation applications. The main objectives of the program are: *i*) to reduce the cost of the Pt catalyst and ionomeric membrane, *ii*) to enhance the efficiency and the power density of PEM fuel cells, *iii*) to define the humidification

conditions that allow long-term operation at high current densities, and *iv*) to achieve good performance in cells operating on reformed methanol and air. The activities in 1989 have been devoted primarily to the development and characterization of electrodes based on low Pt loadings, evaluation of cell performance under various operating conditions, characterization of the membrane, and development and evaluation of methods to increase the CO tolerance of anodes.

Electrode Characterization and Optimization in PEM Fuel Cells. Two PEM fuel cells employing Nafion 117 membrane and electrodes with a Pt loading of 0.175 mg/cm^2, which is half the Pt loading of ordinary Prototech electrodes, were tested. The low-Pt electrodes were prepared by Prototech from carbon cloth material and 20% Pt/C catalyst. The front surface was first "planarized" by filling the gaps in the carbon cloth with carbon powder. A thin layer (nominally 25-μm thick) of a 20% Pt/C catalyst was next applied onto the planarized front surface of the cloth. This mode of preparation was required to ensure that a large fraction of the catalyst is in intimate contact with the ionomeric membrane, in spite of the very small amount of Pt/C powder employed. An additional 50 nm-thick Pt film was sputtered onto the front surface of each electrode prior to cell assembly. This increased the overall Pt loading of the new electrodes to 0.22 mg/cm^2, compared with an overall loading of 0.45 mg/cm^2 in sputter-coated Prototech electrodes tested earlier. The first cell showed a voltage of 0.5 V at 1 A/cm^2 when operating on H_2/O_2 (30/60 psig) at 80°C, and 0.4 V when operating on H_2/air under similar P, T conditions. The second cell exhibited voltages that were lower by ~50 mV at the same current density. For single cells based on Nafion 117 membrane, this performance is almost indistinguishable from that found with cells employing Prototech electrodes with twice the Pt loading. These results clearly show that the Pt loading can be reduced by a factor of two without a significant loss in performance. Past attempts to lower the nominal thickness of the (20% Pt/C) catalyst layer to <50 μm always resulted in a loss of activity. The success with these new cells is attributed to planarization of the front surface of the carbon cloth with carbon powder prior to the application of the thin layer of Pt/C catalyst.

AC impedance measurements were conducted on single PEM fuel cells operating under the ordinary single-cell testing conditions. These measurements are the first conducted on PEM fuel cells based on the same graphite hardware employed in the single-cell testing facility, and conducted at fuel cell operating temperatures and pressures. Impedance measurements on cathodes in operating fuel cells clearly identified that, at lower potentials (high cathode overpotentials), a well-resolved arc appears in the impedance spectrum at low frequencies. The impedance at low frequency increases in magnitude at higher cathode overpotential. This behavior has been shown to result from mass transport limitations in a thin film through which the gaseous reactant must diffuse to reach the catalyst. Another possible reason for a greater than linear voltage loss at high current densities in similar cells has also been identified. The cathode impedance plots at the highest current densities (lowest cathode potentials) in some cells show a gradual increase in the high frequency intercept. The high-frequency impedance increases, *e.g.*, from 0.24 ohm-cm^2 at the lowest cell current (at 0.9 V) to 0.34 ohm-cm^2 at the highest cell current (at 0.2 V). This behavior is expected when the cell current causes an increase in the membrane resistance. The membrane resistance would increase with current density if "drag" of water by the protonic current brought about local dehydration in the ionomeric membrane near the anode. What the impedance results have demonstrated is that cell losses can originate from flooding phenomena in the cathode catalyst layer and from dehydration phenomena in the membrane, both problems occurring simultaneously at high current densities.

Fuel Cell Structure and Fuel Cell Operating Conditions. In 1989, LANL attained, for the first time, current densities >2 A/cm^2 in PEM fuel cells with low Pt loadings and 50-μm thick Nafion membranes. The results showed that the cell voltage fell from ~0.4 to 0 V as the current density increased from 2 to 3.2-3.4 A/cm^2. Measurements of the cell voltage and anode overpotential indicated that the decrease in voltage at >2 A/cm^2 originates from losses at the cathode. It is remarkable that such high current densities can be obtained from an air cathode with such low Pt loading. The structure of the carbon cloth in the Prototech electrode must be an important factor in determining the electrode performance. To the best of our knowledge, such current densities have not been achieved in other PEM fuel cells based on high Pt catalyst loadings and operated on air. It should be stressed that this high current density is only obtained in PEM fuel cells with thin (50-μm thick) membranes. With these thin membranes, the high-frequency resistance (RHF) is 0.14-0.15 ohm-cm^2 as compared with 0.27-0.32 ohm-cm^2 in cells with Nafion 117 membranes. This low level of RHF was subsequently repeated in single cells with "Membrane C" produced by Chlorine Engineers Corp., Japan. This is a perfluorinated sulfonic acid membrane with an equiva-

lent weight of 900 and a thickness of ~125 μm in the dry state. Hot-pressing of the membrane-electrode assembly at a temperature of 145°C, instead of the usual temperature of 135°C, produced good performance. In addition, good reproducibility in the performance of 5-cm^2 cells based on "Membrane C" has been obtained. This reproducibility can be judged by comparing specific points along the polarization curve, as summarized in the following table.

Cell Voltages (uncorrected)
or Three Cells Based on Membrane C

Current Density (mA/cm^2)	Uncorrected Cell Voltage (V)					
	Cell 76		Cell 85		Cell 86	
	Oxygen	Air	Oxygen	Air	Oxygen	Air
500	0.77	0.72	0.75	0.70	0.75	0.70
1000	0.67	0.60	0.64	0.54	0.66	0.55
1500	0.57	0.42	0.53	0.33	0.55	0.30
2000	0.42	–	0.40	–	0.40	–

The cathode gas pressure in these measurements was 60 psig, and the anode gas pressure was 30 psig. The high-frequency resistance in these cells was 0.12–0.16 ohm-cm^2, *i.e.*, comparable in values to those cells obtained with 50-μm Nafion membranes. Several factors may be responsible for the reproducible performance in cells with membrane C: *i*) optimization of the hot-pressing conditions, *ii*) the superior properties of this membrane with regard to bonding to the carbon cloth, and *iii*) less shape change in the membrane during dry-wet cycles.

Membrane Properties – Water Drag Measurements. The water drag in membranes was measured under conditions that more closely resemble those encountered in operating fuel cells. An earlier cell

$$H_2O, Pd(H)/Nafion/Pd(H), H_2O$$

was modified to a new design

$$H_2O, Pd(H)/Nafion/Pt, H_2$$

This latter cell has one compartment filled with H_2O while the other compartment is filled with humidified hydrogen gas that reacts electrochemically at a gas diffusion Pt/C Prototech electrode (hot-pressed onto the ionomeric membrane). The rise or fall of H_2O in a capillary attached to the liquid-filled compartment provides information on the net transport of H_2O between the two compartments as a result of the passage of protonic current. The results obtained with this new cell showed a net transport of only about 0.5 H_2O molecules per proton from the anode to the cathode compartment. Furthermore, the measured transfer of H_2O seems to fall in consecutive experiments with protonic current of the same polarity. The most probable reason for the relatively small amount of H_2O transport following the replacement of H_2O on the anode side by humidified hydrogen is a lowered hydration level on the anode side under the latter conditions. A further issue with the Pd(H)/ionomer membrane/Pd(H) assembly immersed in H_2O has been the effect of the nature of the ionomeric membrane. The H_2O drag by protons at room temperature was measured with several membranes in the earlier cell, and the following results were obtained:

Membrane	Water Drag, H_2O/H^+
Nafion 117	2.5-2.9
Experimental Membrane X	1.5-1.8
Recast Nafion	2.9-3.4
Membrane C	2.6-4.1

The drag through Membrane X (unknown EW) at room temperature is about half that of the drag through the Nafion membrane. This could be one reason for the higher performance observed in PEM fuel cells with Membrane X, which produces a smaller rate of H_2O removal from the anode side at high current densities. On the other hand, Membrane C exhibits larger (and rather unstable) H_2O drag. Both Membrane C and Membrane X have lower equivalent weights than Nafion 117 (Membrane C has an EW of 900), but the trend of the drag, as compared with that in Nafion 117, is different — smaller in the Membrane X material and larger in Membrane C. This must mean that factors other than the EW affect the level of H_2O drag.

A measurement of H_2O mass balance in a 50-cm^2 single PEM fuel cell was completed. The goal of the experiment was to check if a mass balance in the amount of H_2O entering the cell, of H_2O generated within the cell, and of H_2O exiting the cell could be demonstrated under conditions of constant cell current. The experiments were performed with Kynar-impregnated graphite current collector plates of relatively low porosity. The results of the experiments are summarized in the following table.

Hydrogen Flow:	300 cm^3/min
Oxygen Flow:	150 cm^3/min
Gas Pressure:	1 atm
Cell Temperature:	80°C
Humidifier Temperature:	80°C
Water Measurements:	
From anode exhaust (open circuit):	6.67 g/hr
From cathode exhaust (open circuit):	2.79 g/hr
From anode exhaust (500 mA/cm^2):	3.02; 3.32 g/hr*
From cathode exhaust (500 mA/cm^2):	15.49; 15.10 g/hr*

* Duplicate experiments.

The total amount of H_2O generated in the cell by passing a current of 25 A is calculated to be 8.39 g/hr, which is lower than the measured values of 9.05 and 8.96 g/hr (two experiments). The distribution of the H_2O between the anode and cathode exhaust showed that some H_2O drag occurs from the anode to cathode. The anode is missing about 3.5 g/hr as a result of current passage, all of which appears in the cathode exhaust. This level of H_2O transfer from anode-to-cathode compartment corresponds to a drag of 0.2 H_2O/H^+. A similar experiment was subsequently performed with the humidifier temperature higher than that of the cell (T_{cell}/T_{hum} = 80°C/90°C). In this case, the H_2O content in the gas streams was found to be much higher than expected for H_2O in the vapor phase alone. This must mean that a substantial amount of H_2O is "entrained" by the gas passing through a humidifier held at 90°C. These results suggest that the single cells are usually operated with a large excess of H_2O, which enters the cell in the form of an aerosol. This enhances the conductivity of the ionomeric components but could cause cathode flooding problems, particularly when operating on air.

CO Poisoning. Tests of the effects of 100-ppm CO in the anode feed stream showed that CO poisoning is smaller at high fuel utilization levels (when the fuel stoichiometry approaches 1). At high fuel flow rates (low utilization) the performance degradation caused by 100-ppm CO is severe, whereas at low flow rates (stoichiometry between 1.2 and 1.5) the performance degrades slowly. In either case, the injection of 2% O_2 into the anode feed stream resulted in complete recovery in performance. The relative improvement at low stoichiometry could be caused, in principle, by a non-equilibrium coverage by CO or by partial elimination of CO from the gas. An analysis of the fuel exhaust gas was undertaken to distinguish between these two possibilities. The gas sample was collected in an infrared cell with an adjustable optical path length up to 20 meters. The analysis of the anode exhaust, collected from a single cell operating on H_2 containing 95-ppm CO (H_2 flow stoichiometry of 3) showed a drop in the level of CO and an increase in the level of CO_2, both brought about by just passing the CO-contaminated H_2 through the anode compartment of the cell. (In this experiment, no O_2 was added to the anode feed stream). These results indicate that a substantial lowering of the CO level in the anode gas mixture occurs in the anode compartment. The most plausible mechanism for this is permeation of O_2 through the membrane from the cathode to anode side. This O_2 would react with adsorbed CO, just as it does when O_2 is intentionally injected into the anode. The amount of O_2 permeation depends on the oxygen partial pressure at the cathode and on the possible presence of flaws (*e.g.*, pinholes) in the membrane. The infrared spectrum of the anode exhaust stream obtained when 2% O_2 was added to the CO-contaminated H_2 feed showed that the CO is completely eliminated from the gas mixture. These results indicate that the rate of chemical oxidation of CO at the anode catalyst, in the presence of 100-ppm CO and 2% O_2, is sufficient to lower the partial pressure of CO in the gas mixture to practically zero, thereby completely eliminating the effects of poisoning.

PUBLICATIONS

1. I.D. Raistrick, T.E. Springer, R. Sherman, and S. Gottesfeld (1989), "Kinetics of Oxygen Reduction and Hydrogen Oxidation at the Platinum/Ionomeric Membrane Interface," *175th Meeting of the Electrochemical Society*, Los Angeles, CA, Abstract No. 571.
2. S. Gottesfeld (1989), "Fuel Cells Based on the Direct Oxidation of Methanol," *175th Meeting of the Electrochemical Society*, Los Angeles, CA, Abstract No. 317.
3. C.R. Derouin, J. Pafford, S. Radzinsky, T.E. Springer, and S. Gottesfeld (1989), "Processes in Ionomeric Membranes Employed in Proton-Exchange (PEM) Fuel Cells," *175th Meeting of the Electrochemical Society*, Los Angeles, CA, Abstract No. 627.
4. M.T. Paffett, B.E. Koel, and S. Gottesfeld (1989), "Fundamental Electrochemical and Surface Science Studies of Cooxidation at Polycrystalline Pt Surfaces," *175th Meeting of the Electrochemical Society*, Los Angeles, CA, Abstract No. 459.

5. E.A. Ticianelli, J.G. Beery, M.T. Paffett, and S. Gottesfeld (1989), "An Electrochemical, Ellipsometric, and Surface Science Investigation of the PtRu Bulk Alloy Surface," *J. Electroanal. Chem.* **265**, 15.
6. W. Paik, T.E. Springer, and S. Srinivasan (1989), "Kinetics of Fuel Cell Reactions at the Platinum/Solid Polymer Electrolyte Interface," *J. Electrochem. Soc.* **136**, 644.
7. T.E. Springer and I.D. Raistrick (1989), "Electrical Impedance of a Pore Wall for the Flooded-Agglomerate Model of Porous Gas-Diffusion Electrodes," *J. Electrochem. Soc.* **136**, 1594.

Advanced Chemistry and Materials for Fuel Cells

J. McBreen (Brookhaven National Laboratory)

The purpose of this work is to increase the understanding of electrocatalysis on a molecular level and to apply this knowledge to fuel cells. The goals of this project are to reduce the Pt requirements in PEM fuel cells, and to develop non-Pt catalysts for O_2 reduction and the direct oxidation of methanol. Work in 1989 included EXAFS studies of *i*) Pt supported on carbon in acid electrolytes, *ii*) UPD Cu and Pb on Pt supported on carbon catalysts, and *iii*) pyrolyzed FeTMPP and CoTMPP on high-surface-area carbon.

EXAFS Studies of UPD Cu, H and Pb on Pt. Adsorbed submonolayers of foreign metal atoms are known to catalyze methanol oxidation. EXAFS studies were conducted to determine the structure of these adsorbates and the nature of the catalytic effects. The first experiments were x-ray absorption near edge structure (XANES) studies of UPD Cu on Pt supported on carbon at 50 mV *vs* SCE in 1 N H_2SO_4. The XANES spectra were obtained at both the Cu and Pt edges. The results indicate that the adsorbed Cu has a Cu(I) oxidation state. With the adsorption of Cu there is a concomitant filling of the d-bands of Pt. This causes a decrease in the Pt XANES white line. In pure acid electrolytes there is a broadening of the Pt XANES white line in the hydrogen adsorption region. This indicates that the adsorbed hydrogen is hydridic in nature and that there is a partial emptying of the d-bands of the Pt. The adsorption edge for UPD Pb on Pt in 1 M $HClO_4$ is between that for Pb foil and PbO. This indicates the non-metallic nature of UPD Pb. The non-metallic nature of UPD Cu was also confirmed by EXAFS measurements. The interaction of Cu with both Pt and O could be clearly seen. The catalytic effects of UPD layers must be related to the electronic effects on the Pt and interaction of the UPD metals with O species in the electrolyte.

EXAFS Studies of Pyrolyzed Macrocycles. EXAFS studies of pyrolyzed FeTMPP (900°C) and CoTMPP (800°C) were extended to include SEXAFS studies at the nitrogen edge. No evidence of any nitrogen was found. This confirmed prior XPS results. It must be concluded that no nitrogen is present and that previous models based on nitrogen-containing residues are incorrect. The EXAFS results will have to be analyzed again with carefully chosen reference compounds. The Fourier transform of the EXAFS for pyrolyzed FeTMPP on Vulcan XC-72 only displayed one peak just below 0.2 nm. Much higher concentrations and much better spectra were obtained on Cabot Black Pearls carbon. In this case the Fourier transform displayed a second peak above 2 nm. The significance of this is not known. All of this indicates that much more experimental work and data analysis are needed to elucidate the structure of these catalysts.

PUBLICATIONS

1. J. McBreen, W.E. O'Grady, G. Tourillon, E. Dartyge and A. Fontaine (1989), "In-Situ XANES Study of UPD Copper on Carbon Supported Platinum," *175th Meeting of the Electrochemical Society*, Los Angeles, CA, Abstract No. 547.

LAWRENCE BERKELEY LABORATORY
UNIVERSITY OF CALIFORNIA
INFORMATION RESOURCES DEPARTMENT
BERKELEY, CALIFORNIA 94720